

## Accepted Manuscript

Cave ventilation and rainfall signals in dripwater in a monsoonal setting - a monitoring study from NE India

Sebastian F.M. Breitenbach, Franziska A. Lechleitner, Hanno Meyer, Gregory Diengdoh, David Matthey, Norbert Marwan

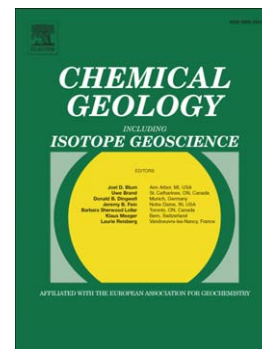
PII: S0009-2541(15)00145-X  
DOI: doi: [10.1016/j.chemgeo.2015.03.011](https://doi.org/10.1016/j.chemgeo.2015.03.011)  
Reference: CHEMGE 17530

To appear in: *Chemical Geology*

Received date: 1 October 2014  
Revised date: 8 March 2015  
Accepted date: 10 March 2015

Please cite this article as: Breitenbach, Sebastian F.M., Lechleitner, Franziska A., Meyer, Hanno, Diengdoh, Gregory, Matthey, David, Marwan, Norbert, Cave ventilation and rainfall signals in dripwater in a monsoonal setting - a monitoring study from NE India, *Chemical Geology* (2015), doi: [10.1016/j.chemgeo.2015.03.011](https://doi.org/10.1016/j.chemgeo.2015.03.011)

This is a PDF file of an unedited manuscript that has been accepted for publication. As a service to our customers we are providing this early version of the manuscript. The manuscript will undergo copyediting, typesetting, and review of the resulting proof before it is published in its final form. Please note that during the production process errors may be discovered which could affect the content, and all legal disclaimers that apply to the journal pertain.



**Cave ventilation and rainfall signals in dripwater in a monsoonal setting – a monitoring study from NE India**

Sebastian F.M. Breitenbach<sup>1,\*</sup>, Franziska A. Lechleitner<sup>2</sup>, Hanno Meyer<sup>3</sup>, Gregory Diengdoh<sup>4</sup>, David Matthey<sup>5</sup>, Norbert Marwan<sup>6</sup>

<sup>1</sup> Sediment and Isotope Geology, Ruhr-Universität Bochum, Institute for Geology, Mineralogy & Geophysics, Universitätsstr. 150, 44801 Bochum, Germany (formerly Department of Earth Science, Eidgenössische Technische Hochschule (ETH), CH-8092 Zürich, Switzerland)

<sup>2</sup> Department of Earth Science, Eidgenössische Technische Hochschule (ETH), CH-8092 Zürich, Switzerland

<sup>3</sup> Alfred Wegener Institute for Polar and Marine Research, Telegrafenberg, 14473 Potsdam, Germany

<sup>4</sup> Pansy Cottage, Mission Compound, 793002 Shillong, Meghalaya, India

<sup>5</sup> Department of Earth Sciences, Royal Holloway University London, Egham, UK

<sup>6</sup> Potsdam Institute for Climate Impact Research, 14412 Potsdam, Germany

\*Corresponding author: Email: breitenbach@speleo-berlin.de; Address: Sediment and Isotope Geology, Ruhr-Universität Bochum, Institute for Geology, Mineralogy & Geophysics, Universitätsstr. 150, 44801 Bochum, Germany; Tel: +492343223255; Fax: +492343214571

**Highlights:**

- Mawmluh Cave dripwater bears monsoonal rainfall signal
- Ventilation depends on surface-cave temperature gradient and river flow
- Dry season cave air CO<sub>2</sub> is closely linked to gas transport via entrances and less to soil air CO<sub>2</sub>
- Evidence suggests anthropogenic impact on aquifer, temperature, and ventilation dynamics

**Keywords:** Indian Summer Monsoon, microclimate monitoring, water isotopes, cave ventilation

## Abstract

Detailed monitoring of subterranean microclimatic and hydrological conditions can delineate factors influencing speleothem-based climate proxy data and helps in their interpretation. Multi-annual monitoring of water stable isotopes, air temperature, relative humidity, drip rates and  $P_{CO_2}$  in surface, soil and cave air gives detailed insight into dripwater isotopes, temperature and ventilation dynamics in Mawmluh Cave, NE India.

Water isotopes vary seasonally in response to monsoonal rainfall. Most negative values are observed during late Indian Summer Monsoon (ISM), with a less than one-month lag between ISM rainfall and drip response. Two dry season and two less-well distinguishable wet season dynamic ventilation regimes are identified in Mawmluh Cave. Cave air temperatures higher than surface air result in chimney ventilation during dry season nights. Dry season days show reduced ventilation due to cool cave air relative to surface air and cold-air lake development. Both, high water flow and cooler-than-surface cave air temperatures result in air inflow during wet season nights. Wet season daytime ventilation is governed by river flow, but is prone to stagnation and development of cold air lakes.  $CO_2$  monitoring indicates that  $P_{CO_2}$  levels vary at diurnal to annual scale. Mawmluh Cave seems to act as  $CO_2$  sink during part of the dry season. While very likely, additional data is needed to establish whether wet season cave air  $CO_2$  levels rise above atmospheric values. Drip behavior is highly nonlinear, related to effective recharge dynamics, and further complicated by human influence on the epikarst aquifer.

## 1 Introduction

### 1.1 Importance of cave microclimate monitoring

Speleothems grow as secondary carbonate precipitates in caves, incorporating information on surface conditions from the dripwater feeding them. Precise dating with the U/Th method and a multitude of geochemical proxies incorporated in speleothem carbonate can provide reconstructions of past climatic and environmental change at exceptional resolution and quality (Johnson et al. 2006, Matthey et al. 2008, Ridley et al. 2015).

Speleothem growth is influenced by numerous cave-specific factors, and exact reconstructions of past climate conditions from stalagmite proxy records critically depend on detailed observations of the local surface environment, the karst aquifer hydrology and the cave microclimate. Local vegetation, and soil type, bedrock lithology, cave morphology and seasonal conditions are known to strongly affect proxy signal transfer from surface to cave. Additionally, prior calcite precipitation (PCP), cave ventilation and drip rate changes in the karst system have been recognized as important processes influencing both isotope and trace element signatures (Fairchild & Baker 2012).

Cave microclimate monitoring helps understanding these processes and is especially important when proxy time series are calibrated against meteorological records to derive transfer functions for quantification of climatological parameters (e.g. temperature or rainfall amount) (Matthey et al. 2008, 2010). The increasing number of sub-annually resolved paleoclimate records (Treble et al. 2003, Johnson et al. 2006, Ridley et al., in press) also requires excellent chronological control and detailed dripwater monitoring to understand the exact timing of proxy signal incorporation into the speleothem carbonate (Shen et al. 2013). Cave microclimate monitoring studies have been reported from different climatic settings in Europe (Pflitsch & Piasecki 2003, Spötl et al. 2005, Boch et al. 2010, Matthey et al. 2010, Frisia et al. 2011), North America (Oster et al. 2012), Australia (McDonald et al. 2007) and East Asia (Hu et al. 2008, Partin et al. 2012). However, lack of long-term observations from monsoonal India complicates the assessment of the ISM core region response to global climate change.

In this article, we present multi-annual cave monitoring data from Mawmluh cave in Meghalaya, northeastern India, where record ISM rainfall is observed (Prokop & Walanus 2003). We show that strong seasonality in the isotope composition of ISM precipitation is retained in the dripwater with a lag of less than one month, allowing high-frequency climate reconstructions with stalagmites from this cave. Cave ventilation affects CO<sub>2</sub> dynamics and thus speleothem growth and  $\delta^{13}\text{C}_{\text{speleothem}}$ . We develop a conceptual model to describe the influence of multiple physical parameters, as cave ventilation, on climatically relevant proxies from stalagmites. Importantly, this model is likely valid in many

other (sub-)tropical settings experiencing high seasonality and similar ventilation regime.

Our data further suggests alterations in epikarst hydrology, ventilation, and temperature dynamics related to quarrying and deforestation. Human activity above the cave might have severe repercussions on the cave habitat and proxy-calibration.

### 1.2 Cave ventilation

The exchange of cave air with the surface atmosphere (ventilation) directly affects temperature, humidity and cave air  $P_{CO_2}$  dynamics. In conjunction with dripwater chemistry, it exerts a first-order control on the growth conditions and isotopic and element signature in speleothems (Dreybrodt 1988, Baldini et al. 2006, 2010, Banner et al. 2007, Matthey et al. 2010, Ridley et al. in press). Cave ventilation is driven by diurnal to inter-seasonal and even inter-annual variations in air density gradients between surface and cave air. These variations can result from differential warming between surface and cave, as well as from air pressure changes and water flow conditions (Baker & Fairchild 2012).

These parameters influence the water-solid phase fractionation during carbonate precipitation (Fairchild & Baker 2012, Baldini et al. 2010, Frisia et al. 2011). Cave air  $P_{CO_2}$  directly affects dripwater pH and  $CO_2$  degassing, and thus stalagmite growth rates and carbon isotope and element signatures (Banner et al. 2007, Mühlinghaus et al. 2007, Matthey et al. 2008). Similarly, cave air temperature variations affect evaporation from droplets and stalagmite surfaces, modulating isotope fractionation processes (Mühlinghaus et al. 2007, 2009). Modeling and laboratory studies confirm that drip rate variations might strongly affect isotope characteristics (Day & Henderson 2012, Mühlinghaus et al. 2007). Detailed monitoring of these parameters helps establishing which forcing factors govern geochemical variability in dripwater and speleothem carbonate.

## 2 Study Area

### 2.1 Geographical and climatological setting

The Meghalaya Plateau is a 1,200 to 1,700 m high west-east oriented mountain ridge north of Bangladesh (Fig. 1). Its morphology is the result of tectonic uplift

of the detached Indian plate north of the Dauki fault (Biswas and Grasemann 2005). The region is characterized by high seismic activity related to the northward movement of the Indian plate. The southern rim of the plateau is built up by Tertiary sediments, mostly conglomerates, sandstones, coal and limestones. The region is known to receive the World's highest amount of annual rainfall, but precipitation is distinctly seasonal. The ISM delivers 75-85% of annual rainfall between June and October (Breitenbach et al. 2010a, Prokop & Walanus 2003), while frequent water shortage occurs on the plateau during the dry season (Breitenbach et al. 2010b).

The peculiar climate conditions are mirrored by the geomorphology of the Meghalaya Plateau. Excessive ISM rainfall results in substantial erosion along the southern plateau margin, development of spectacular gorges that cut northward into the plateau (Fig. 1B), and intense karstification of the limestone deposits.

**Fig. 1 Overview maps of study region.** A) Mawmluh Cave is located at the southern fringe of the Meghalaya Plateau in NE India. The study area receives moisture mainly from the Bay of Bengal. B) Record monsoonal rainfall results in intense erosion and development of deep gorges. Mawmluh Cave developed in a butte on the very margin of the plateau. SRTM global topography data is available from the U S Geological Survey (<http://seamless.usgs.gov/>) and shown as shaded relief map using software Fledermaus. The relief is vertically 4x exaggerated. C) Red circles indicate sampling locations in Mawmluh Cave. The river is shown in blue, flowing from the main entrance towards the northeastern section of the cave. The monitored and sampled parameters are color coded as shown in the legend. Cave survey, profile and plan view modified after Gebauer (pers. comm. 2014).

## 2.2 Mawmluh Cave

Mawmluh Cave is located on the southern fringe of the Meghalaya Plateau (25°15'32"N and 91°42'45"E; Figs. 1A, B). The main entrance is located at 1,160 m above sea level (asl), while additional entrances are found in dolines, e.g. in the 'Goldfish Pond doline' (GPD) at 1,129 m asl (Fig. 1C). The cave developed as complex subhorizontal system along the contact between the ~9 m thick dolomitic Lakadong member of the Sylhet Limestone formation and the Therria Sandstone (both Lower Eocene, Gogoi et al. 2009). At present, it is a 7 km long maze following Mawmluh River, which sinks into the main entrance (Fig. 1C). Importantly, the 'Hanging Gardens' (HG) passage is much larger (ca. 5-8 m wide and 2-4 m high) compared to 'Candle Highway' (CH) passage (1.5 m wide and 0.5 to 5 m high), which is reached through a very narrow squeeze. The cave is

overlain by 30-100 m thick and heavily karstified host rock consisting of limestone, sandstone, and a 40-100 cm thick coal layer. Only a very thin soil (5-15 cm) covers the host rock, with grasses and bushes as main vegetation. Evergreen forest is found in the moisture- and shadow-providing dolines. The industrial-grade limestone and coal found on top of the dolomitic Lakadong limestone are quarried for a cement factory that has been established in 1966. Mining activity and the factory itself have detrimental effects on Mawmluh Cave. Blasting has collapsed a main passage, and the river is heavily polluted with oil, gasoline and other effluences from the factory. Mawmluh Cave is the focus of palaeoclimate and microbiological research, making it an important site for detailed cave monitoring studies (Baskar et al. 2008, Biswas et al. 2009, Berkelhammer et al. 2012, Breitenbach et al. 2012a, 2012b, Lechleitner et al. 2012, Myers et al., in revision).

### 3 Instrumentation and Methodology

#### 3.1 Meteorological data

To relate seasonal microclimatic parameters monitored in Mawmluh Cave to surface conditions we used daily rainfall and temperature data from the nearby Cherrapunji meteorological station ([www.cherrapunjee.com/weather\\_info.php](http://www.cherrapunjee.com/weather_info.php)). Rainfall and temperature recorded at 30 min intervals between 2010 and 2014 in Mawmluh village (located ~1.5 km from the cave, 1,247 m a.s.l.) are used for the study of diurnal variability. Details on instrumentation are given in supplemental table 1.

#### 3.2 Stable isotopes in river and cave water

Drip and river water samples have been collected for stable isotope analysis ( $\delta^{18}\text{O}$  and  $\delta\text{D}$ ) at several locations (Fig. 1C) near and in Mawmluh Cave between March 2011 and March 2014 at roughly monthly intervals. Due to flooding of several passages during the ISM season we were unable to obtain samples for July. Sampling encompassed the Mawmluh River at the main cave entrance (CE) and in the HG, as well as dripwater in HG and CH. Dripwater was collected as monthly batch samples with a 1L plastic bottle and as direct grab samples from feeding soda straws whenever drip rates allowed. All samples were collected in

airtight plastic and glass bottles and stored in dark and cool conditions before transfer to the laboratory. 89 samples were analyzed at the Alfred-Wegener-Institute Potsdam, Germany (Table 1). The stable isotope composition was determined using the method detailed in Meyer et al. (2000) and results are reported in permil (‰) relative to the Vienna Standard Mean Ocean Water (VSMOW) standard.

### 3.3 Cave air temperature and humidity

Temperatures (T) have been recorded between March 2007 and March 2014 at 30-minute intervals, with several gaps that resulted from battery or instrument failures. Instruments were installed in the GPD cave entrance, in HG and the CH meander using automatic logging instruments (Tinytag Plus 2, [www.tinytag.info](http://www.tinytag.info) and HOBO® ProV2, [www.onsetcomp.com](http://www.onsetcomp.com)) (Fig. 1C).

Manual spot humidity measurements were performed during fieldwork in March 2007, April 2009 and March 2014. Readings were obtained using a handheld aspiration psychrometer (VEB Messgeräte Mitte, Berlin, GDR). Wet and dry thermometer readings and relative humidity were recorded after rotating the psychrometer for at least three minutes. Individual spot air temperature measurements with the same instrument correspond closely to instrumental readings from the automatic loggers (within  $\pm 0.7^{\circ}\text{C}$ ).

### 3.4 Air CO<sub>2</sub> analysis

Cave air  $P_{\text{CO}_2}$  has been manually measured in 2009, 2012 and 2014, while automatic logging began in March 2014. Single measurements in 2009 were performed using a Vaisala MI70 indicator coupled to a Vaisala GMP343 Carbocap CO<sub>2</sub> probe with a precision of  $\pm 10\%$ . Subsequent measurements were conducted using a non-dispersive infrared monitoring device (CORA) with a long-term precision of  $\pm 1.6\%$  and an accuracy of  $\sim \pm 3\%$  (Luetscher & Ziegler 2012). Measurements were carried out in HG and CH and are currently continued in CH (Fig. 1C). Additionally, samples of surface, cave and soil air were collected for CO<sub>2</sub> abundance using a low flow pump to fill 1L or 3L Tedlar bags at a rate of 200 ml/minute. Cave air spot measurements and sampling was carried out as the first task in each chamber to avoid contamination by respired CO<sub>2</sub>. A soil air

collection site was prepared above the cave for gas analysis using porous PTFE sampling cups (Ecotech, Germany) buried at 70 cm and 25 cm.

### 3.5 Drip rates

Automatic acoustic stalagmite drip loggers (Collister & Matthey 2008) were installed below two drip sites in CH. One drip logger was placed in a beaker outfitted with an outlet for parallel water collection for monthly isotope samples (Drip A). A second logger of the same type was placed ca. 2 m away from drip A below a soda straw without beaker (Drip B). Both loggers recorded the number of drip events over 30 minutes periods. We calculate daily discharge ( $Q$  in L/day) by assuming a volume of 0.23 ml/drip (Collister & Matthey 2008).

## 4. Results

### 4.1 Local Meteorological data

Temperatures in Mawmluh village and at the meteorological station in Cherrapunji are very similar ( $R^2=0.86$ ), and show substantial variations in annual surface temperature between 4°C to 35°C (Fig. 2). The high-resolution monitoring data allows comparing surface and cave conditions and diurnal ventilation dynamics. Diurnal temperature cycles are most pronounced during the dry season (up to 20°C), whereas summers are characterized by generally high air temperature with very limited nighttime cooling (diurnal amplitude ~4-6°C) (Fig. 3).

Daily data from Cherrapunji meteorological station show annual rainfall ranging from 7,560 mm in 2013 to 13,472 mm in 2010. ISM (JJAS) rainfall contributes the largest fraction to annual rainfall, although varying widely from 58% to 87% between 2009 and 2013.

**Fig. 2 Meteorological characteristics at the surface and inside Mawmluh Cave.** A) Cave air temperature has been monitored in CH since March 2007 and in HG and GPD since 2010. Daily minimum and mean temperature are available for Cherrapunji meteorological station since 2009. GPD temperature varies with surface air temperature. B) Temperature difference (daily) between cave (CH) and Cherrapunji ( $\Delta T_{CH-Cherra}$ ) and GPD and Cherrapunji ( $\Delta T_{GPD-Cherra}$ ) help delineating direction of airflow. Positive  $\Delta T_{CH-Cherra}$  during the dry winter initiates chimney ventilation out of the cave, while negative summertime  $\Delta T_{CH-Cherra}$  limits ventilation.  $T_{GPD-Cherra}$  changed significantly since 2012, concurrently with deforestation in the doline. C) Cave air relative humidity (RH) is variable and frequently found below saturation. Blue shading indicates wet ISM seasons.

**Fig. 3 Diurnal temperature variability in Mawmluh Cave and Mawmluh village.** **A)** Dry season temperature at the GPD entrance varies on diurnal scale in line with surface air temperature in the village, albeit largely attenuated. At the same time diurnal variations disappear almost entirely inside the cave, although small temperature changes can be observed on weekly to monthly scale. **B)** While wet season temperature is higher compared to the dry season, its variability is suppressed at the surface and at the cave entrance. Diurnal variations are found at HG, while at CH almost constant temperatures are recorded.

#### 4.2 Stable isotopes in river and cave water

Oxygen isotope ratios in river water inside Mawmluh Cave range from  $-7.0\text{‰}$  to  $-4.7\text{‰}$ , while the surface river shows larger variability between  $-8.9\text{‰}$  and  $-4.8\text{‰}$  (Fig. 4A, Table 1). Hydrogen isotope compositions inside and outside the cave range from  $-43.4\text{‰}$  to  $-23.8\text{‰}$  and from  $-60.4\text{‰}$  to  $-27.1\text{‰}$ , respectively (Table 1). External errors ( $1\sigma$ ) for standard measurements were better than  $0.8\text{‰}$  for hydrogen and  $0.08\text{‰}$  for oxygen. Minimum values for both,  $\delta^{18}\text{O}$  and  $\delta\text{D}$ , are observed in August and September (ISM season). Maximum values are recorded during the dry season in March and April.

Cave water samples are statistically indistinguishable from the Local Meteoric Water Line (LMWL, Fig. 4B, Breitenbach et al., 2010a) while surface river water samples sometimes show values below the LMWL. The linear regression of cave dripwaters (cave water line, CWL) can be described as  $\delta\text{D} = (8.23 \pm 0.41) * \delta^{18}\text{O} + (14.02 \pm 2.63)$ ,  $N=73$ ,  $R^2=0.96$ ). Cave water  $\delta$  excess varies from  $4.9\text{‰}$  to  $15.8\text{‰}$  around an average value of  $12.6 \pm 1.0\text{‰}$ .

**Fig. 4 Stable isotope signature of surface river and Mawmluh Cave waters between 2011 and 2014.**

**A)** Cave water  $\delta^{18}\text{O}$  varies  $\sim 2\text{‰}$  seasonally, while surface river water (at CE) shows a larger range of  $4\text{‰}$ . Lowest  $\delta^{18}\text{O}$  values are observed during the ISM seasons (grey shaded). **B)** Cave waters plot close to the LMWL determined by Breitenbach et al. (2010a). Several surface river water samples are located below the LMWL and reflect signs of evaporation. The Cave Water Line (CWL) is indistinguishable from the LMWL.

#### 4.3 Cave air temperature

Air temperature at the GPD entrance has been monitored between January 2010 and March 2014 (Fig. 2A) and strong annual cycles are observed, with temperature varying between  $6.8$  and  $23.5^\circ\text{C}$ . Lowest values are recorded

between December and March, while highest temperatures occur during the ISM season (June to October). The temperature difference between GPD and Cherrapunij ( $\Delta T_{\text{GPD-Cherra}}$ ) also displays annual cycles (Fig. 2B). Between 2010 and early 2012 the difference values were generally negative, with an annual amplitude of  $\sim 10^\circ\text{C}$ , varying between  $-9^\circ\text{C}$  and  $+1^\circ\text{C}$ . The doline remained almost always cooler than the plateau, with equal to slightly higher values during the ISM season.

A sudden positive shift in both dry season minimum and wet season maximum GPD temperatures is observed after the dry season 2011-2012. This shift to higher values is also observed in  $\Delta T_{\text{GPD-Cherra}}$ , reflecting a severe warming of the doline by several degrees. The annual amplitude increased to  $15^\circ\text{C}$ , now ranging from  $-6^\circ\text{C}$  to  $+9^\circ\text{C}$ . Today the doline is colder than the plateau only in winter, while during summer it is often significantly warmer.

Although no data was recorded between December 2012 and March 2013 it is apparent that the dry season minima showed a relatively stable mean temperature of  $\sim 9^\circ\text{C}$  between 2009 and 2012, while since 2012 the minima were significantly higher ( $\sim 12^\circ\text{C}$ ). Similarly, summer season maxima increased from a mean of ca.  $19.5^\circ\text{C}$  in the period 2010-2011 to an average of  $\sim 21.5^\circ\text{C}$  in 2012 and 2013. A change in the summer temperature profile from a plateau-like maximum to a skewed shape can be discerned.

Diurnal cycles in the doline are dampened and lag temperature changes in the village by one to three hours. The cycles are well expressed during the dry season (Fig. 3A), while during the ISM the amplitude is suppressed (Fig. 3B).

Inside Mawmluh Cave temperature variations are close to the mean annual temperature ( $\text{MAT}_{\text{Mawmluh Village}} = 19^\circ\text{C}$ ), with seasonal variability decreasing to  $0.7^\circ\text{C}$  in the more secluded CH passage (Fig. 2A). Temperature in HG passage varies up to  $3.6^\circ\text{C}$  over the period of a year, with evidence for some inter-annual variability. The strong attenuation of temperature variability can be attributed to restricted ventilation, which results in prolonged temperature equilibration between air and host rock in this narrow passage. CH temperature varied very regularly between March 2007 and December 2011, ranging  $\sim 0.8^\circ\text{C}$  around a mean of  $18.5^\circ\text{C}$ , very similar to the average temperature at Cherrapunji meteorological station and Mawmluh village for the same period. The

temperature difference between CH and Cherrapunji ( $\Delta T_{\text{CH-Cherra}}$ ) varied  $\sim 16^{\circ}\text{C}$  at annual scale and shows negative values during the ISM season (the cave being colder than the plateau). Between 2010 and 2012 wet season  $\Delta T_{\text{CH-Cherra}}$  remained relatively stable with values around  $-2^{\circ}\text{C}$ . In 2012 a negative trend set in, which resulted in almost two degrees cooling in CH between summer 2011 and 2013, coinciding with GDP warming. This trend is mirrored by  $\Delta T_{\text{CH-Cherra}}$ , averaging  $-4^{\circ}\text{C}$  in summer 2013.

Very small diurnal temperature changes with variable amplitudes on the order of  $0.1$  to  $0.2^{\circ}\text{C}$  (within instrumental uncertainty) are found in HG, while no diurnal response is observed in CH (Fig. 3). The amplitude of the diurnal cycles in HG varies seasonally; while during the dry season it might vary  $<0.1^{\circ}\text{C}$  (Fig. 3A), the range increases to  $\sim 0.3^{\circ}\text{C}$  during the ISM season (Fig. 3B). At monthly and longer timescales, both HG and CH respond to variations in surface air temperature. Due to larger passage dimensions this response is faster and more pronounced in HG compared to CH, i.e. HG temperature sinks lower in dry season and rises higher in wet season (Fig. 3B).

#### 4.4 Relative humidity

Given the limited available data we can only tentatively discuss RH dynamics in Mawmluh Cave. All measurements were taken during the dry season. Dry season RH varies from 68 to 100% at Hanging Gardens (Fig. 2C). Although no data is available for the ISM season we assume that the rise of the cave river by several meters, higher drip rates and a waterlogged epikarst lead to RH close to 100% between June and September.

#### 4.5. $\text{CO}_2$

$\text{CO}_2$  data is summarized in table 2. Three sampling methods were employed: on-site spot measurements, collection in sampling bags and subsequent laboratory analysis, and continuous logging. In April 2009,  $P_{\text{CO}_2}$  was only slightly elevated in HG (490 ppm) relative to outside air, while it was higher in CH (630 ppm). The highest  $P_{\text{CO}_2}$  level has been observed in May 2012 (1049 ppm). Similar slightly elevated values were also observed in the bag samples returned for laboratory analysis.

A week-long high-resolution (30-min intervals) monitoring campaign in HG between 3<sup>rd</sup> and 10<sup>th</sup> of March 2014 revealed substantially lower  $P_{CO_2}$  ( $168 \pm 8$  ppm) in Mawmluh Cave (Fig. 5). The high-resolution experiment exhibits diurnal-scale cyclic  $CO_2$  variations with amplitudes of  $\sim 10$  ppm, and higher values during the night. The temperature time series does not show diurnal cycles and the high frequency variability seen in Figure 5 is probably instrumental noise (instrumental accuracy is  $\pm 0.2^\circ C$ ). Comparing the measurements from April 2009, May 2012 and March 2014 suggests that  $P_{CO_2}$  levels vary strongly, depending on ventilation conditions, with higher values in the late pre-monsoon season.

Dry season soil  $CO_2$  levels are highly variable and vary between 441 and 5936 ppm (table 2). No wet season data is available due to waterlogging of the soil, but intense vegetation activity likely leads to high soil  $CO_2$  levels.

**Fig. 5 Dry season  $P_{CO_2}$  levels in Mawmluh Cave, HG passage.** High resolution monitoring in March 2014 shows that  $CO_2$  concentration varies at diurnal to weekly time scales.  $CO_2$  is significantly correlated with cave air temperature (inset). Diurnal  $P_{CO_2}$  variations are superimposed on the long-term trend. Note that temperature variations are minimal ( $< 0.1^\circ C$ ). The data can be found in supplemental table 1.

#### 4.6 Drip rates

Drip rates recorded between January 2010 and August 2013 show strong variability, with daily discharge ranging from 0 to 23.9 L/day (Drip A) and 0.06 to 32.5 L/day (Drip B) (Fig. 6). A clear relationship between drip rates in Mawmluh Cave and rainfall at Cherrapunji cannot be discerned. Although a very general trend to higher drip rates during and after the summer monsoon is observed, a distinct response to ISM rainfall is not found. While highest drip rates in July/August 2012 and May/June 2013 roughly correspond to the respective ISM seasons, very high drip rates can also appear during the dry seasons, for example during the dry season 2010-2011 and in February 2012. These drip signals do not correspond to the ISM season and drip rates seem unrelated to rainfall events. Lowest drip rates are generally recorded between March and May, but with high variability. The lag in drip rate as response to increased rainfall is difficult to assign, but is unlikely to exceed one month, as

evidenced by dripwater isotopes, which show lowest values in the post-monsoon periods (Fig. 6). The annual variations of  $\delta^{18}\text{O}$  in dripwater and local rainfall correspond closely, suggesting short delays in the arrival of surface water at drip sites.

**Fig. 6 Relationship between Mawmluh drip activity (at CH) and rainfall.** Daily drip rates from CH are compared with weekly rainfall from the meteorological station at Cherrapunji and isotope data from drips in the same passage. Somewhat higher drip rates are found during and after the ISM. Dry season drip rates diminish between March and May, but with strong variability. Dripwater  $\delta^{18}\text{O}$  is lowest in the late and early post monsoon.

## 5 Discussion

### 5.1 $\delta^{18}\text{O}$ and $\delta\text{D}$ in river and dripwater

The isotope signature of water near and inside Mawmluh Cave is governed by the Indian summer monsoon (ISM), as it delivers most of the annual rainfall. Rainwater isotopes in Meghalaya are strongly depleted during the ISM, due to increasing distance of the moisture source, variations in moisture transport pathway, and changes in Bay of Bengal surface water (Breitenbach et al. 2010a). River water in Meghalaya carries the integrated isotope signature of local precipitation in the respective drainage basin (Ernst et al. 2013), a finding confirmed by our analysis of surface river water at site CE (Fig. 7). The seasonal variability of CE river water  $\delta^{18}\text{O}$  and  $\delta\text{D}$  is very similar to that of precipitation (Breitenbach et al. 2010a), with most depleted values in October (late ISM season) and highest values in February (dry season). The fast return to less negative  $\delta^{18}\text{O}$  values in November, after the end of the ISM, agrees well with the notion of a fast response in the small drainage basin of Mawmluh River. CE water samples plot on the Local Meteoric Water Line reported by Breitenbach and coworkers (2010a). Four samples show slight secondary evaporation effects, slightly reducing slope and intercept in the  $\delta^{18}\text{O}$ - $\delta\text{D}$  diagram. These four samples stem from the dry season and show low  $d$  excess values, underlining the importance of re-evaporation from surface and stream water for the isotopic composition of recharge in the area (Kendall & Coplen 2001).

Dripwater samples collected in CH and HG show a distinct seasonal pattern (Fig. 7), with highest values in January and lowest in October. This seasonal isotope

signature with a skewed minimum at the end of the ISM season is very similar to that observed in rainfall, suggesting quick transfer of rainfall to the cave, with a lag of less than one month. The range in dripwater  $\delta^{18}\text{O}$  from  $-7\text{‰}$  to  $-5.5\text{‰}$  is evidence for a bias towards ISM rainfall, which has a mean  $\delta^{18}\text{O}$  value around  $-7\text{‰}$  (Breitenbach et al. 2010a), and possibly some buffering in the epikarst. Minimal effective infiltration during the dry season results in only part of the strongly enriched rainwater ( $\delta^{18}\text{O}_{\text{mean}}$  ca.  $-2\text{‰}$ ) to be delivered into the cave, and the dripwater isotope signature is dominated by ISM rainfall.

The fact that all dripwater samples are located on the Local Meteoric Water Line (Fig. 4B) suggests that evaporation is not an important process affecting dripwater, which robustly represents ISM moisture. Higher resolution sampling would be necessary to define the exact lag between rainfall and the response of the dripwater with regard to their stable isotope signature. Since seasonal oxygen isotope variations are recovered from dripwater in Mawmluh Cave we anticipate that seasonally resolved stalagmite isotope records can be obtained if stalagmite growth rates are sufficiently high (Myers et al., in revision).

**Fig. 7 Average precipitation, river water and dripwater  $\delta^{18}\text{O}$ .** Mean dripwater  $\delta^{18}\text{O}$  varies seasonally about  $1.5\text{‰}$ , while average  $\delta^{18}\text{O}$  of river water collected at the surface at CE shows  $\sim 2.5\text{‰}$  of variability. Lowest values are recorded during the ISM between August and October, congruent to rainfall  $\delta^{18}\text{O}$ . Rainwater data (presented on a different y-axis) are average monthly data for 2007 and 2008, taken from Breitenbach et al. 2010a.

## 5.2 Doline and cave air temperature

From 2010 and until summer 2012, air temperature in GPD remained near the lower end of surface air temperature as recorded in Cherrapunji and Mawmluh Village (Fig. 2A). The  $\sim 1.5^\circ\text{C}$  temperature increase since 2012 can be explained by a drastic reduction in forest cover in the doline. Since summer 2012 partial deforestation has been observed in the doline, mostly for firewood collection by the local population. Reduced forest cover leads to increased heating and stronger evaporation from the soil in the doline, reduced temperature-buffering capacity and higher recorded temperature at the cave entrance.

Cave air temperature was relatively stable between 2007 and 2012, but ongoing cooling set in since summer 2012 (Fig. 2A), coincident with the temperature shift

in the doline. This suggests a direct response of cave air temperature and, possibly ventilation dynamics to surface changes.

Short-term (diurnal-scale) temperature variations diminish with distance from the cave entrance and passage size. Deeper and more secluded passages also show an increasing lag in their response to external temperature changes (Fig. 3A). Both phenomena are clearly related to reduced air exchange in more distant and secluded passages. Additional variability in the thermal regime in HG results from the river flowing through this passage.

### 5.3 Cave meteorology and ventilation

Ventilation in Mawmluh Cave can be classified as dynamic, with significant changes at seasonal to diurnal scale. We distinguish four ventilation regimes: dry season and wet season ventilation, each separated into night and day regimes (Fig. 8).

Ventilation dynamics are influenced partly by temperature-induced air density differences between cave and surface. The complex cave geometry with several entrances and a  $\sim 30$  m altitude difference between CE and GPD strongly influences airflow direction and velocity by introducing a chimney effect (Pflitsch & Piasecki 2003, Spötl et al. 2005, Fairchild & Baker 2012, Ridley et al. in press). Additionally, strong river flow can induce air velocities proportional to that of the stream via friction between water and air (Cigna 1968, Fairchild & Baker 2012). Mawmluh River modulates the otherwise density-driven system and leads to suction of air through and out of the cave, mainly during the ISM season. Air density variations, chimney effect and water-induced flow together govern ventilation dynamics in Mawmluh Cave.

Ventilation and water play an important role for the  $\text{CO}_2$  dynamics in Mawmluh cave, as the  $\text{CO}_2$  budget might be strongly influenced by dolomite weathering (Liu & Zhao 1999), and possibly  $\text{CO}_2$ -absorption by river (e.g. Baldini et al. 2006), pool, and condensation water. Low  $\text{CO}_2$  production in the overlying soil during the dry season (table 2) aggravates the scarcity of  $\text{CO}_2$  in the epikarst and cave. Given the low observed  $P_{\text{CO}_2}$  levels the influence of the cave air  $\text{CO}_2$  partial pressure on buoyancy and ventilation is negligible (Sánchez-Cañete et al. 2013).

Advective air and heat transport depend on the temperature gradient between surface and cave, as cool dense air moves downward, while warm and less dense air rises. Mawmluh village and Cherrapunji meteorological station (both at similar altitudes relative to the cave) are used as reference sites for plateau temperatures. We use  $\Delta T_{\text{CH-Cherra}}$  and  $\Delta T_{\text{GPD-Cherra}}$ , based on daily surface and cave air temperature data to determine periods of inward and outward airflow. Daily temperature data from Cherrapunji rather than Mawmluh village are used because this dataset is more complete and both are significantly correlated ( $R^2=0.89$ ).

### 5.3.1 Dry season ventilation

Low surface air temperatures result in almost continuously positive  $\Delta T_{\text{CH-Cherra}}$  values between October and March (Fig. 2B). At the same time,  $\Delta T_{\text{GPD-Cherra}}$  shows negative values, most likely due to the doline's secluded geometry, which acts as cold air trap. The positive temperature difference between cave and plateau (Fig. 8A) and the  $\sim 30$  m altitude difference between CE and GPD allows the development of a chimney effect, as enhanced inflow of cool surface air from lower entrances into the cave while warm cave air exits via the cave's upper entrances (Pflitsch & Piasecki 2003).

Figure 8A illustrates nocturnal ventilation in Mawmluh Cave during the dry season. In the afternoon and early night cave air temperature is higher than at the surface (positive  $\Delta T_{\text{CH-village}}$ , see also Fig. 9A), initiating outward ventilation via high entrances. The fact that GPD temperature remains lower than cave and plateau indicates that GPD is not the exit route for warm air from the cave. Intensified inward airflow during the night allows suction of surface air and addition of atmospheric  $\text{CO}_2$ , reflected in increasing cave air  $P_{\text{CO}_2}$  and slight lowering of cave air temperature. Exemplary data from March 2010 are also presented in Fig. 9A.

**Fig. 8 Schematic representation of ventilation conditions in Mawmluh Cave during dry and wet season (day and night).** **A)** Dry season nights are characterized by low surface and higher cave air temperature, allowing air to exit the cave through the upper entrance (chimney effect). This leads to influx of surface air and  $\text{CO}_2$ -enrichment of cave air. **B)** In the morning hours cold air limits the chimney effect and ventilation is minimized. Cave air  $\text{CO}_2$  decreases due to weathering and absorption. **C)** Wet season nights are

characterized by high surface and slightly lower cave air temperatures, inhibiting chimney-driven ventilation. High river discharge through the cave pulls surface air into the cave, freshening the cave.  $\text{CO}_2$  increases due to high  $\text{CO}_2$  flux from soil and epikarst and possibly river degassing, likely leading to higher than atmospheric  $P_{\text{CO}_2}$ . Cave air can exit via lower exits, e.g. Goldfish Pond Doline, due to reduced cave-surface temperature difference. **D)** During the day high surface and low cave air temperatures support stagnant conditions, but high river discharge leads to influx of surface air.  $\text{CO}_2$  remains high and no significant airflow into GPD is detected, probably due to low  $\Delta T_{\text{CH-village}}$ .

The ventilation regime changes in the morning hours as outlined in Figs. 8B and 9A. High daytime surface air temperature and cool cave air lead to negative  $\Delta T_{\text{CH-village}}$  values, weakening the chimney effect and minimizing outward airflow via CE. The relatively cooler and denser cave air could either exit via low cave entrances or become stagnant in a cold air lake. The former is unlikely, since GPD temperature increases slightly over the day, but remains colder than both cave and plateau. Cave air pressure, recorded parallel to  $\text{CO}_2$ , shows two daily maxima, possibly indicating a change in airflow direction. This feature could be explained by a regime shift from chimney flow (towards CE) to river-induced flow (towards low entrances), albeit at minor scale as indicated by decreasing  $P_{\text{CO}_2}$  (see below).

Since 2012 the dry season regime has undergone significant changes, likely related to the onset of deforestation in the doline. Data from March 2013 show a drastic lowering in cave air temperature  $T_{\text{CH}}$  and its variance, concurrent with an increase in doline temperature (Fig. 9B). These changes are accompanied by a significant lowering of nighttime  $\Delta T_{\text{CH-village}}$ , minimizing chimney-driven ventilation.

Decreasing  $P_{\text{CO}_2}$  levels in the cave over the day (Fig. 5) support the notion of stagnant conditions and minimal airflow. Prolonged  $\text{CO}_2$  absorption from the slow-moving or stagnant cave air by carbonate weathering and potentially river and ponded water might explain the low cave air  $P_{\text{CO}_2}$ . The effectiveness of these processes is amplified by low  $\text{CO}_2$  production in the overlying soil and limited supply of surface air with atmospheric  $\text{CO}_2$ . Cave air is replenished with surface air  $\text{CO}_2$  when cool air enters the cave during the night. The ongoing alteration in the ventilation pattern is likely to reduce nighttime air exchange, possibly resulting in lower  $P_{\text{CO}_2}$  levels due to diminished replenishment with fresh air.

### 5.3.2 Wet season ventilation

During the ISM  $\Delta T_{\text{CH-Cherra}}$  is mostly negative, and cave and surface air temperature are relatively close, with 1-5°C difference on average (e.g. in July 2010). Chimney effect-driven ventilation is minimized and cool stagnant air could accumulate in the cave, were it not for the drastically increased river discharge. The river running through Mawmluh Cave rises several meters during the ISM season, changing passage volume and discharge and injecting warm surface air into the cave. The epikarst is quickly filled with infiltrating rainwater, further limiting air exchange through the host rock. The ventilation then tends to shift from an exogenic to an endogenic system (*sensu* Pflitsch & Piasecki 2003) driven by stream flow and down-river air current. The wet season can be characterized by two diurnal scale ventilation regimes, although both appear very similar due to river influence (Fig. 8C and D).

Nocturnal wet season ventilation is characterized by only slightly negative  $\Delta T_{\text{CH-Mawmluh}}$  values (ca. -1.2°C), since summer night temperatures are close to cave air temperature (Fig. 9C). Density-driven rise of cave air is limited by minimal  $\Delta T_{\text{CH-Village}}$ . Air is entrained by the fast flowing river from the upper entrance and exits at the lower entrances (Fig. 8C), a scenario corroborated by observed temperature dynamics in GPD.  $\Delta T_{\text{CH-GPD}}$  increases during the night, indicating cool cave airflow into GPD (Fig. 9C).

Over the day surface air temperature increases only slightly and when low cloud cover allows direct surface warming. The cave then is significantly cooler relative to the surface ( $\Delta T_{\text{CH-Village}}$  increases) and the chimney effect is minimized (Figs. 8D, 9C). The stream, entraining air at CE, mainly drives ventilation downstream. The stream seems to have little effect on GPD, where stable daytime temperatures are recorded. The large temperature difference between cave and surface air ( $\Delta T_{\text{CH-Village}}$ ) also favors stagnation of ventilation, as discussed below. Highly variable stream level and speed,  $\Delta T_{\text{CH-Village}}$ , as well as potential additional factors (e.g. air pressure changes related to storms etc.) probably result in unstable and variable summertime ventilation conditions.

The temperature regime has changed markedly since 2012 and much lower  $\Delta T_{\text{CH-Village}}$  values were observed in 2013 (Figs. 3 and 9D). Temperature differences between cave and surface are largely driven by surface temperature variability, while the cave remains colder than both, GPD and village. The

observed warming in GPD and contemporaneous cooling at CH can be best explained by evaporational cooling inside the cave as a direct response to altered ventilation, which itself results from deforestation in the doline.  $\Delta T_{\text{GPD-Cherra}}$  increased strongly since 2012 as a result of intensified doline deforestation. A dense canopy of tropical forest acts as buffer against evapotranspiration, cooling the air in the doline. If denuded of its forest cover, the doline can warm faster, as observed after the start of deforestation. The temperature changes shown in figure 9D illustrate the ventilation mechanism at diurnal scale: GPD and CH temperatures show very little diurnal variability around 22°C and 16.8°C respectively, while air temperature in the village varies between 20 and 26°C. This means that  $T_{\text{CH}}$  is always coldest, while  $T_{\text{GPD}}$  is higher than  $T_{\text{village}}$  during nighttime and lower during the day. Warm nighttime GPD air rises and is replenished by cave air (i.e. outward ventilation is enhanced). This ventilation in turn intensifies evaporational cooling inside the cave (Cuthbert et al. 2014), visible in progressively more negative nighttime  $\Delta T_{\text{CH-GPD}}$  (Fig. 9D). The absolute temperature differences ( $\Delta T_{\text{CH-GPD}}$  and  $\Delta T_{\text{CH-village}}$ ) increase with warming of plateau and GPD in the morning. When the plateau becomes warmer than the doline (negative  $\Delta T_{\text{GPD-village}}$ ) upward airflow from the doline falters and the cave ventilation effect is slackened.

Over longer periods, the deforestation-driven intensification of ventilation leads to progressive evaporational cooling, expressed by decreasing  $T_{\text{CH}}$  since 2012. This anthropogenically induced process will likely affect carbonate precipitation (evaporation enhances oversaturation and thus carbonate precipitation) and carbonate oxygen isotope signatures (Cuthbert et al. 2014). Lower cave air temperature also increases the potential for development of a cold air lake in the cave with stagnant air (Fig. 8D).

Although no  $\text{CO}_2$  data is currently available we assume that  $\text{CO}_2$  influx to the cave is maximized during the ISM season, when the site receives world-record rainfall amounts (Prokop & Walanus 2003). Concomitantly, biomass production is strongly enhanced (Ramakrishnan 1988) and soil and root respiration intensify (Khiewtam & Ramakrishnan 1993). High  $\text{CO}_2$  production in the soil would enhance dripwater  $\text{CO}_2$  (Figs. 8C, D); observed higher cave air  $\text{CO}_2$  concentration of 1049 ppm in mid-May 2012 supports this notion. Additional  $\text{CO}_2$  might be

delivered from degassing of the stream (Troester and White 1984). Then, in-cave  $P_{CO_2}$  level is likely higher than during the dry season, although possibly highly variable, depending on high frequency changes in ventilation regimes.

**Fig. 9 Comparison of temperature dynamics in different seasons.** **A)** Daily dry season varied  $>20^{\circ}C$  on the plateau ( $T_{Village}$ ),  $<2^{\circ}C$  in the doline ( $T_{GPD}$ ) and only  $\sim 0.05^{\circ}C$  in CH ( $T_{CH}$ ).  $\Delta T_{CH-Village}$  and  $\Delta T_{GPD-Village}$  are positive during the night and strongly negative over the day.  $\Delta T_{CH-GPD}$  is positive, highest during the night and varies  $\sim 1-1.5^{\circ}C$ . **B)** In March 2013  $T_{GPD}$  increased by  $\sim 2^{\circ}C$ , while  $T_{Village}$  was similar to 2010. At the same time  $T_{CH}$  decreased  $\sim 1.5^{\circ}C$ , resulting in reduced difference between GPD and Mawmluh village (lower nighttime  $\Delta T_{GPD-Village}$ ) and lower  $\Delta T_{CH-GPD}$ . **C)** The ISM season 2010 showed very stable surface and cave temperature conditions. Nighttime  $\Delta T_{CH-Village}$  was only slightly negative, while during the day it showed minimum values of ca.  $-5^{\circ}C$ .  $\Delta T_{GPD-Village}$  followed closely, although with  $1^{\circ}C$  higher values.  $\Delta T_{CH-GPD}$  was highest during the night. **D)** In July 2013  $T_{Village}$  showed somewhat higher diurnal variability ( $5^{\circ}C$ ) while  $T_{GPD}$  was stable, albeit at a higher level. Thus  $\Delta T_{GPD-Village}$  was higher, with positive values during nighttime, facilitating the rise of doline air.  $T_{CH}$  was  $1.9^{\circ}C$  lower than in 2010.  $\Delta T_{CH-Village}$  and  $\Delta T_{GPD-Village}$  were more negative, with lowest values during the day. This reflects faster response of doline temperature to surface warming as direct result of deforestation. Lower  $\Delta T_{CH-Village}$  during dry and ISM season hamper chimney-driven circulation.

### 5.3.3 Ventilation influence on dripwater $CO_2$ degassing and speleothem isotopy

$CO_2$  degassing from dripwater entering a cave roof depends mainly on the  $CO_2$  gradient between water and cave air. The concentration of dissolved  $CO_2$  in dripwater is generally much higher than cave air  $P_{CO_2}$  (Baldini 2010), and degassing from the drip occurs immediately upon entering the cave. Low cave air  $P_{CO_2}$  can maximize carbonate precipitation rates, although other factors, e.g. water hardness, can modify this mechanism (Baldini 2010, Spötl et al. 2005). The degassing rate also determines the degree of kinetic fractionation of carbon (and to some degree oxygen) isotope composition (Spötl et al. 2005, Mühlinghaus et al. 2007, 2009). Low cave air  $P_{CO_2}$ , combined with low drip rates lead to prolonged degassing and increasing  $\delta^{13}C_{speleothem}$ .

Seasonal  $P_{CO_2}$  dynamics in Mawmluh Cave might be a likely cause for the high speleothem deposition rates ( $>250\mu m/a$ ) and the growth of annual laminae in modern speleothems (Myers et al., in revision). Observed laminae are composed of couplets of dense, translucent and more fragile milky-white aragonite crystals. As outlined in fig. 10, low dry season cave air  $P_{CO_2}$  enhances dripwater  $CO_2$  degassing, resulting in faster growth of milky-white porous aragonite and less negative  $\delta^{13}C$ . If our assumption of high wet season  $P_{CO_2}$  is true, wet season

stalagmite growth would be limited due to reduced CO<sub>2</sub> degassing, resulting in thin dense translucent layers with low  $\delta^{13}\text{C}$ . Wet season  $\delta^{18}\text{O}$  is more negative due to ISM influence (Fig. 7). This mechanism is likely functional in other (sub-)tropical cave settings with similar seasonality.

The influence of ventilation on the growth and isotope composition of speleothems is confirmed by sub-seasonal data, which shows high  $\delta^{13}\text{C}$  and  $\delta^{18}\text{O}$  values within white and lower values in the dark laminae (Myers, pers. comm.).

**Fig. 10 Conceptual summary of the influence of natural parameters on stalagmite growth and isotope composition in Mawmluh Cave.** Seasonal changes in CO<sub>2</sub> degassing and rainfall  $\delta^{18}\text{O}$  govern growth pattern and  $\delta^{13}\text{C}$  and  $\delta^{18}\text{O}$  variability in stalagmites in Mawmluh Cave.

Anthropogenic or natural alteration of the natural ventilation system is likely to affect speleothem geochemistry. The trend to reduced air exchange in Mawmluh Cave during both dry and monsoon season following the onset of deforestation in 2012 could increase CO<sub>2</sub> seasonality. Reduced dry season ventilation allows intensified CO<sub>2</sub> absorption, leading to even more depleted cave air  $P_{\text{CO}_2}$  during the dry season. Carbonate deposition in the wet season might well increase, with higher  $\delta^{18}\text{O}$  and reduced seasonality in the isotopic signature in speleothems. Additional detailed monitoring is required to unravel the link between deforestation and ventilation dynamics and the cave's response to these changes in near future.

#### 5.4 CO<sub>2</sub> in Mawmluh Cave

Cave air CO<sub>2</sub> analyses show that cave  $P_{\text{CO}_2}$  levels are seasonally highly variable and only moderately elevated above background atmosphere. Our data indicate that lowest  $P_{\text{CO}_2}$  values during the dry season. Rising cave air CO<sub>2</sub> levels are observed towards the wet season in late May, but variability remains high (e.g. the  $P_{\text{CO}_2}$  level in April 2010 in CH was 876 ppm while it was 443 ppm in HG, compared to 1049 ppm in HG two years later). The highly dynamic nature of  $P_{\text{CO}_2}$  at our study site is also reflected in soil data, which range from 468 ppm to 5936 ppm at 75 cm depth in the same month of the dry season (table 2).

The high-resolution measurements from HG show  $P_{\text{CO}_2}$  below ambient surface air values (Fig. 5), which hints to extraction of  $\text{CO}_2$  in the cave during the dry season. Instrumental errors are unlikely the reason for the observed low values, as the instrument correctly show atmospheric  $P_{\text{CO}_2}$  values at the surface before deployment in Mawmluh cave. However, long-term measurements are needed to substantiate these measurements.

#### 5.4 Drip rates

Drip rate behavior in Mawmluh Cave was monitored to study its influence on  $\text{CO}_2$  degassing and isotopic fractionation during carbonate precipitation (Day and Henderson 2012, Mühlinghaus et al. 2007).

Drip rate changes in Mawmluh Cave do not simply reflect monsoonal rainfall variations. Comparison of drip and rainfall data from Cherrapunji suggests that while drip sites in CH are generally sensitive to rainfall events this sensitivity varies over the year. Drips respond quickly on rain spells if the water reservoir in the epikarst has been depleted before during a prolonged dry period (e. g. between the late dry season and the onset of the ISM season). Under such conditions the monitored drips show very short lag periods (<1-3 weeks), hinting to substantial conduit and fracture flow components (Fairchild & McMillan 2007). Once the epikarst is waterlogged after early monsoonal rainfall, drip sensitivity diminishes; not all rainfall maxima are then readily translated into higher drip rates and the lag between rainfall and drip rates increases.

The refill of the epikarst reservoir can also lead to prolonged elevated drip discharge. This effect is evident during the ISM season 2011 (Fig. 6), when a pronounced drip rate maximum is found in October and November, after the rainfall abated in September. This behavior can be explained by the limited outflow from the epikarst. If the reservoir is not replenished, drip rates decrease steadily and under dry conditions the drip will slow and its activity might even cease.

While drip discharge increase during early wet season is readily explained by a response to the ISM onset, the active and highly variable drip behavior during the dry season suggests that additional influencing factors complicate the cave's hydrological dynamics. Effective recharge dynamics and epikarst flow regimes

might lead to highly nonlinear behavior in the monitored drip sites (Baker & Brunsdon 2003, Fairchild & Baker 2012). However, these factors seem insufficient to explain the observed high dry season drip discharge variations (as for example at the end of November 2012, Fig. 6). We hypothesize that drip rates react on human activity above the cave. Limestone and coal mining in the quarries above and NE of Mawmluh Cave severely alter the local geomorphology and hydrology, disrupting recharge pathways randomly and unpredictably. Blasting in these quarries (detonations have been felt in the cave during fieldwork) likely affects the aquifer (Biswas 2009) and might trigger erratic drip discharge. Frequent earthquakes in the region might constitute an additional factor altering drip behavior. Such disturbances seem to obliterate any direct drip response to rainfall. For example, high drip rates are recorded during the core dry season (18.10.2010-18.03.2011), when only 148.8 mm of rainfall occurred in the area (Fig. 6). We thus argue that modern drip rate data from Mawmluh Cave are not straightforward interpretable in terms of weather conditions.

Monitoring reveals that the dripwater retains the isotopic signature of ISM rainfall, allowing the reconstruction of monsoonal conditions. Lower  $\delta^{18}\text{O}$  in stalagmites can be directly related to ISM dripwater isotope signatures. Higher  $\delta^{18}\text{O}$  values in Mawmluh speleothems result mainly from decreasing influence of ISM water during progressing dry periods and additionally from open system conditions in the soil and epikarst, rather than longer drip intervals (Mühlinghaus et al. 2009) (Fig. 10).

Drip discharge dynamics affect dripwater  $\text{CO}_2$  degassing and carbon isotope fractionation during carbonate precipitation, especially at high temperatures and low drip rates and humidity (Day and Henderson 2012, Mühlinghaus et al. 2007). Speleothem  $\delta^{13}\text{C}$  will be lower during the wet season due to the combined effects of increased drip discharge and  $\text{CO}_2$  levels, which reduce fractionation effects on  $\delta^{13}\text{C}$  (Fig. 10). High  $\delta^{13}\text{C}$  values result from enhanced  $\text{CO}_2$  degassing and associated carbon isotope fractionation during dry periods with lower cave air  $P_{\text{CO}_2}$ . Although additional factors might further complicate the picture, this mechanism explains the covariance in speleothem  $\delta^{13}\text{C}$  and  $\delta^{18}\text{O}$  at seasonal scale. On inter-decadal to millennial scale, factors, such as changes in vegetation

density and composition must be considered. The impact of large-scale natural vegetation dynamics on speleothem isotope composition could be tested using modern anthropogenic deforestation as analogue.

## 6 Conclusions

A multiyear monitoring study, initiated in 2007 in Mawmluh Cave, NE India gives detailed insight into the processes that govern cave ventilation and dripwater isotope dynamics. The study included monitoring of dripwater stable isotopes, air temperature, relative humidity,  $P_{CO_2}$  in surface, soil and cave air, and drip rates. A small catchment and high permeability of the strongly fractured host rock results in short residence time of infiltrating water. This allows rapid signal transfer from the surface into the cave, making Mawmluh Cave very sensitive to environmental changes. Our main findings can be summarized as follows:

- Dripwater  $\delta^{18}O$  and  $\delta D$  vary at seasonal scale and are closely related to monsoonal rainfall. Most negative isotope values are observed during late ISM, congruent with the isotope signature in precipitation. This observation suggests a signal transfer time of less than one month from surface to cave. Speleothem-based isotope time series can therefore give valuable insights into ISM dynamics at seasonal scale.
- Temperature and  $CO_2$  monitoring reveals four natural dynamic ventilation regimes in Mawmluh Cave. Cave air temperatures warmer than surface air and chimney ventilation characterize dry season nights, while during dry season days cave air is cooler than surface air, leading to reduced ventilation and potentially the development of a cold air lake. Wet season ventilation is characterized by very high stream water flow and cave air temperatures colder than at the surface, resulting in downstream airflow. This river flow based ventilation regime is most pronounced during nighttime, whereas during daytime this ventilation regime is slackened due to larger cave-surface temperature differences and cold air lake development.

Deforestation in the doline above the cave affects temperature regimes and ventilation dynamics, likely altering growth and isotope pattern in speleothems. Additional data is needed to unravel the magnitude of human impact on the cave environment.

- Detailed knowledge about the cave air CO<sub>2</sub> dynamics is vital to understand isotope fractionation processes during speleothem formation. Preliminary results from CO<sub>2</sub> monitoring indicate highly dynamic  $P_{\text{CO}_2}$  levels, with variations at diurnal to annual scale. The data suggest that Mawmluh Cave acts as CO<sub>2</sub> sink during part of the dry season. We assume that intense soil activity during the wet season would result in higher cave air CO<sub>2</sub> levels. Available data suggest that in Mawmluh Cave CO<sub>2</sub> degassing from dripwater is variable, leading to seasonally differing carbonate precipitation rates and fractionation conditions.
- Drip rate behavior in Mawmluh Cave is highly nonlinear. The observed variability is related to effective recharge dynamics and epikarst flow regimes, but complicated due to human activity above the cave. We hypothesize that ongoing quarrying affects the overlying aquifer and drip discharge in Mawmluh Cave.
- Mawmluh Cave offers insights into the response of the temperature and ventilation regimes – and by extension carbonate deposition and isotope composition – in a cave subject to human activity (by quarrying and deforestation). Continued monitoring will allow quantification of the response time and magnitude of geochemical alteration in growing speleothems, and improve the interpretation of paleoclimate proxy records.

This study highlights the importance of the many processes involved in altering geochemical signals in speleothems. Ventilation dynamics, rainfall seasonality and human action all influence the caves microclimate and the growth and composition of stalagmites. Thus, long-term observations are vital wherever high-resolution climate reconstructions are attempted using cave deposits, as the influencing processes are ubiquitous, but specific for each case study.

Speleothems from strongly seasonal climates are frequently characterized by high growth rates, allowing sub-annual reconstructions of climate variability. For correct interpretation of such records it is vital to disentangle the governing processes at seasonal scale.

Moreover, the better understanding of anthropogenic impacts on proxy records can help to estimate the impact of past natural large-scale environmental

changes on stalagmite isotope composition. Direct observations of comparable environmental changes are generally not available, comprising important aspects for future research.

### Acknowledgement

Brian Kharpran Daly and Herbert D. Gebauer are gratefully acknowledged for their support during fieldwork and for providing detailed information and cave survey data. We thank Denis Rayen for providing daily meteorological data and Steven Goodbred for DEM data. Rebecca Fisher carried out the air analyses. D.P.M. acknowledges logistical assistance from Talat Ahmed. S.F.M.B. gratefully acknowledges financial and logistical support from the Swiss National Science Foundation, Project STALCLIM (CRSI22\_132646/1). N.M. and S.F.M.B. received support from the German Science Foundation (research group HIMPAC, FOR 1380). N.M. received financial support from the German Science Foundation (DFG project MA 4759/4-1). D.M. and the work carried out at Royal Holloway were supported by NERC grant NE/G010463/1; Rebecca Fisher carried out the air analyses and field data were collected with Nigel Harris (Open University) and Talat Ahmed (University of Delhi). We thank two anonymous reviewers and the editor for their detailed and constructive comments.

### References

- Baker, A., Brunson, C., 2003. Non-linearities in drip water hydrology: an example from Stump Cross Caverns, Yorkshire. *Journal of Hydrology* 277, 151-163
- Baldini, J.U.L., Baldini, L.M., McDermott, F., Clipson, N., 2006. Carbon dioxide sources, sinks, and spatial variability in shallow temperate zone caves: Evidence from Ballynamintra Cave, Ireland. *Journal of Cave and Karst Studies* 68, 4-11
- Baldini, J.U.L., 2010. Cave atmosphere controls on stalagmite growth rate and palaeoclimate records. *In: Pedley, H.M. & Rogerson, M. (Eds.) Tufas and Speleothems: Unravelling the Microbial and Physical Controls*. Geological Society, London, Special Publications, 336, 283-294
- Banner, J., Guilfoyle, A., James, E.W., Stern, L.A., Musgrove, M., 2007. Seasonal

- variations in modern speleothem calcite growth in Central Texas, U.S.A.  
*Journal of Sedimentary Research* 77, 615–622
- Baskar, S., Baskar, R., Lee, N., Theophilus, P. K., 2008. Speleothems from Mawsmai and Krem Phyllut caves, Meghalaya, India: some evidences on biogenic activities. *Environmental Geology* 57, 1169-1186
- Berkelhammer, M., Sinha, A., Stott, L., Cheng, H., Pausata, F.S.R., Yoshimura, K., 2012. An Abrupt Shift in the Indian Monsoon 4000 Years Ago. *Geophysical Monograph Series* 198, 75–87
- Biswas, J., 2009. The biodiversity of Krem Mawkhyrdop of Meghalaya, India, on the verge of extinction. *Current Science* 96, 904-910
- Biswas, S., Grasemann, B., 2005. Quantitative morphotectonics of the southern Shillong Plateau (Bangladesh/India). *Austrian Journal of Earth Sciences* 97, 82–93
- Boch, R., Spötl, C., Frisia, S., 2010. Origin and palaeoenvironmental significance of lamination in stalagmites from Katerloch Cave, Austria. *Sedimentology* 58, 508–531
- Breitenbach, S.F.M., Adkins, J.F., Meyer, H., Marwan, N., Krishna Kumar, K., Haug, G.H., 2010a. Strong Influence of Water Vapor Source Dynamics on Stable Isotopes in Precipitation Observed in Southern Meghalaya, NE India. *Earth and Planetary Science Letters* 292, 212–220
- Breitenbach, S.F.M., Donges, J., Kharpran Daly, B., Kohn, T., Kohn, T., 2010b. Two sandstone caves on the southern edge of the Meghalaya Plateau, India. *Cave and Karst Science* 37, 49–52
- Breitenbach, S. F. M., Lechleitner, F., Plessen, B., Marwan, N., Cheng, H., Adkins, J. F., Haug, G. H., 2012a. Reconstructing monsoon variations in India – evidence from speleothems. Abstract PP13D-02, AGU Fall Meeting, San Francisco
- Breitenbach, S. F. M., Plessen, B., Marwan, N., Adkins, J. F., Haug, G. H., 2012b. The glacial Indian summer monsoon – precipitation changes during Heinrich and D-O events in NE India. *Geophysical Research Abstracts* 14, EGU2012-7138
- Cigna, A.A., 1968. An analytical study of air circulation in caves. *International Journal of Speleology* 3, 41–54
- Collister, C., Matthey, D., 2008. Controls on water drop volume at speleothem drip sites: An experimental study. *Journal of Hydrology* 358, 259–267

- Cuthbert, M.O., Rau, G.C., Andersen, M.S., Roshan, H., Rutledge, H., Marjo, C.E., Markowska, M., Jex, C.N., Graham, P.W., Mariethoz, G., Acworth, R.I., Baker, A. (2014) Evaporative cooling of speleothem drip water. *Scientific Reports* 4, 5162, 1–7.
- Day, C., Henderson, G.M., 2012. Oxygen isotopes in calcite grown under cave-analogue conditions. *Geochimica et Cosmochimica Acta* 75, 3956–3972
- Dreybrodt, W., 1988. Processes in Karst Systems. Series in Physical Environment, Vol. 4, Springer, Heidelberg, 288 pp
- Ernst, N., Peterse, F., Breitenbach, S.F.M., Syiemlieh, H.J., Eglinton, T., 2013. Biomarkers record the environmental changes along an altitudinal transect in the rainiest place on Earth. *Organic Geochemistry* 60, 93–99
- Fairchild, I.J., McMillan, E.A., 2007. Speleothems as indicators of wet and dry periods. *International Journal of Speleology* 36, 69–74
- Fairchild, I.J., Baker, A., 2012. Speleothem Science: From Process to Past Environments. Wiley, 450 pages
- Frisia, S., Fairchild, I.J., Fohlmeister, J., Miorandi, R., Spötl, C., Borsato, A., 2011. Carbon mass-balance modelling and carbon isotope exchange processes in dynamic caves. *Geochimica et Cosmochimica Acta* 75, 380–400
- Gogoi, B., Kalita, K.D., Garg, R., Borgohain, R., 2009. Foraminiferal biostratigraphy and palaeoenvironment of the Lakadong Limestone of the Mawsynram area, south Shillong Plateau, Meghalaya. *Journal of the Palaeontological Society of India* 54, 209–224
- Hu, C., Henderson, G.M., Huang, J., Chen, Z., Johnson, K.R., 2008. Report of a three-year monitoring programme at Heshang Cave, Central China. *International Journal of Speleology* 37, 143–151
- Johnson, K.R., Hu, C., Belshaw, N.S., Henderson, G.M., 2006. Seasonal trace-element and stable-isotope variations in a Chinese speleothem: The potential for high-resolution paleomonsoon reconstruction. *Earth and Planetary Science Letters* 244, 394–407
- Kendall, C., Coplen, T.P., 2001. Distribution of oxygen-18 and deuterium in river waters across the United States. *Hydrological Processes* 15, 1363–1393

- Khiewtam, R.S., Ramakrishnan, P.S., 1993. Litter and fine root dynamics of a relict sacred grove forest at Cherrapunji in north-eastern India. *Forest Ecology and Management* 60, 327–344
- Lechleitner, F.A., Breitenbach, S.F.M., Cheng, H., Adkins, J.F., Plessen, B., Haug, G.H., 2012. The last deglaciation in NE India reconstructed from a stalagmite from Mawmluh cave. *Geophysical Research Abstracts* 14, EGU2012-701
- Liu, Z., Zhao, J. 1999. Contribution of carbonate rock weathering to the atmospheric CO<sub>2</sub> sink. *Encyclopedia of Earth Science. Environmental Geology* 39, 1053-1058
- Luetscher, M., Ziegler, F., 2012. CORA – a dedicated device for carbon dioxide monitoring in cave environments. *International Journal of Speleology* 41, 273–281
- Mattey, D., Lowry, D., Duffet, J., Fisher, R., Hodge, E., Frisia, S., 2008. A 53 year seasonally resolved oxygen and carbon isotope record from a modern Gibraltar speleothem: Reconstructed drip water and relationship to local precipitation. *Earth and Planetary Science Letters* 269, 80–95
- Mattey, D.P., Fairchild, I.J., Atkinson, T.C., Latin, J.-P., Ainsworth, M., Durell, R., 2010. Gibraltar and trace elements in modern speleothem from St Michaels Cave, Seasonal microclimate control of calcite fabrics, stable isotopes. In: Rogerson, M. (Ed.), *Tufas and Speleothems: Unravelling the Microbial and Physical Controls*, 336. Geological Society of London Special Publications, pp. 323–344.
- Meyer, H., Schönicke, L., Wand, U., Hubberten, H.W., Friedrichsen, H., 2000. Isotope Studies of Hydrogen and Oxygen in Ground Ice - Experiences with the Equilibration Technique, *Isotopes in Environmental and Health Studies* 36, 133-149
- Mühlinghaus, C., Scholz, D., Mangini, A., 2007. Modelling stalagmite growth and  $\delta^{13}\text{C}$  as a function of drip interval and temperature. *Geochimica et Cosmochimica Acta* 71, 2780–2790
- Mühlinghaus, C., Scholz, D., Mangini, A., 2009. Modelling fractionation of stable isotopes in stalagmites. *Geochimica et Cosmochimica Acta* 73, 7275–7289

- McDonald, J., Drysdale, R., 2007. Hydrology of cave drip waters at varying bedrock depths from a karst system in southeastern Australia. *Hydrological Processes* 21, 1737–1748
- Myers, C.G., Oster, J.L., Sharp, W.D., Bennartz, R., Kelley, N.P., Covey, A.K., Breitenbach, S.F.M. (in revision) Northeast Indian stalagmite records El Niño dynamics: implications for moisture transport and drought in India.
- Oster, J.L., Montañez, I.P., Kelley, N.P., 2012. Response of a modern cave system to large seasonal precipitation variability. *Geochimica et Cosmochimica Acta* 91, 92–108
- Partin, J.W., Jenson, J.W., Banner, J.L., Quinn, T.M., Taylor, F.W., Sinclair, D., Hardt, B., Lander, M.A., Bell, T., Miklavic, B., Jocson, J.M.U., Taborosi, D., 2012. Relationship between modern rainfall variability, cave dripwater, and stalagmite geochemistry in Guam, USA. *Geochemistry, Geophysics, Geosystems* 13, Q03013
- Pflitsch, A., Piasecki, J., 2003. Detection of an Airflow System in Niedzwiedzia (Bear) Cave, Kletno, Poland. *Journal of Cave and Karst Studies* 64, 160-173
- Prokop, P., Walanus, A., 2003. Trends and periodicity in the longest instrumental rainfall series for the area of most extreme rainfall in the world northeast India. *Geographia Polonica* 76, 23–31
- Ramakrishnan, P.S., Ram, S.C., 1988. Vegetation, biomass and productivity of seral grasslands of Cherrapunji in north-east India. *Vegetatio* 74, 47- 53
- Ridley, H., Asmerom, Y., Baldini, J.U.L., Breitenbach, S.F.M., Aquino, V.V., Pruffer, K.M., Culleton, B.J., Polyak, V.J., Lechleitner, F.A., Kennett, D.J., Zhang, M., Marwan, N., Macpherson, C.G., Baldini, L.M., Xiao, T., Awe, J., Haug, G.H. (2015) Aerosol forcing of the position of the intertropical convergence zone since AD 1550. *Nature Geoscience* 8, DOI: 10:1038/NNGEO2353.
- Ridley, H., Baldini, J.U.L., Pruffer, K.M., Walczak, I.W., Breitenbach, S.F.M. (in press) High resolution monitoring of a tropical cave system reveals dynamic ventilation and hydrologic resilience to seismic activity. *Journal of Cave and Karst Studies*.
- Sánchez-Cañete, E.P., Serrano-Ortiz, P., Domingo, F., Kowalski, A.S., 2013. Cave ventilation is influenced by variations in the CO<sub>2</sub>-dependent virtual temperature. *International Journal of Speleology* 42, 1-8

- Shen, C.-C., Lin, K., Duan, W., Jiang, X., Partin, J.W., Edwards, L.R., Cheng, H., Tan, M., 2013. Testing the annual nature of speleothem banding. *Scientific Reports* 3, 2633
- Spötl, C., Fairchild, I.J., Tooth, A.F., 2005. Cave air control on dripwater geochemistry, Obir Caves (Austria): Implications for speleothem deposition in dynamically ventilated caves. *Geochimica et Cosmochimica Acta* 69, 2451–2468
- Treble, P., Shelley, J.M.G., Chappell, J., 2003. Comparison of high resolution sub-annual records of trace elements in a modern (1911-1992) speleothem with instrumental climate data from southwest Australia. *Earth and Planetary Science Letters* 216, 141-153
- Troester, J.W., White, W.B., 1984. Seasonal fluctuation in the carbon dioxide partial pressure in a cave atmosphere. *Water Resources Research* 20, 153-156

## Tables

**Table 1 Stable isotope data from water samples collected at and in Mawmluh Cave between 2011 and 2014.** The table is organized by sample type and in chronological order.

#	Sample ID	Collection date	Sample type	$\delta^{18}\text{O}$ [‰ VSMOW]	1 $\sigma$ STDEV	$\delta\text{D}$ [‰ VSMOW]	1 $\sigma$ STDEV	d excess
1	14840	18.03.11	CE river	-4.84	0.03	-28.2	0.3	10.5
2	14850	09.04.11	CE river	-6.31	0.01	-37.1	0.4	13.4
3	14902	07.05.11	CE river	-4.88	0.07	-27.1	0.3	12.0
4	14905	18.06.11	CE river	-6.36	0.05	-38.1	0.4	12.8
5	14911	10.09.11	CE river	-8.91	0.06	-60.4	0.4	10.9
6	14917	15.10.11	CE river	-7.23	0.05	-46.1	0.5	11.8
7	14925	23.11.11	CE river	-5.86	0.08	-39.8	0.6	7.0
8	14928	20.12.11	CE river	-5.54	0.04	-36.9	0.4	7.4
9	14934	25.01.12	CE river	-4.91	0.02	-31.5	0.4	7.8
10	22569	11.08.12	CE river	-6.91	0.01	-43.2	0.4	12.1
11	22574	08.09.12	CE river	-6.35	0.03	-40.7	0.3	10.1
12	22567	21.01.13	CE river	-5.96	0.03	-36.6	0.5	11.1
13	24680	23.05.13	CE river	-5.16	0.01	-29.5	0.4	11.8
14	24649	24.08.13	CE river	-8.36	0.03	-56.8	0.3	10.1
15	24655	26.09.13	CE river	-6.17	0.02	-37.8	0.3	11.6
16	24684	02.11.13	CE river	-7.46	0.05	-49.3	0.1	10.4
17	24662	14.12.13	CE river	-6.48	0.06	-43.3	0.3	8.5
18	24672	27.12.13	CE river	-6.19	0.07	-40.7	0.3	8.9
19	24673	27.12.13	CE river	-6.54	0.05	-43.6	0.1	8.8
20	14838	18.03.11	HG stream	-6.68	0.04	-42.9	0.2	10.6
21	17003	18.06.11	HG stream	-6.88	0.02	-43.4	0.2	11.6
22	14910	10.09.11	HG stream	-6.93	0.04	-43.2	0.4	12.2
23	14915	15.10.11	HG stream	-7.01	0.08	-42.7	0.4	13.4
24	14921	23.11.11	HG stream	-6.88	0.06	-41.4	0.4	13.7
25	14927	20.12.11	HG stream	-6.83	0.05	-42.4	0.3	12.3
26	14933	25.01.12	HG stream	-6.76	0.07	-42.6	0.3	11.5
7	16633	15.05.12	HG stream	-4.68	0.05	-23.8	0.2	13.6
28	28174	03.03.14	HG stream	-6.77	0.02	-41.1	0.3	13.1
29	28155	10.03.14	HG stream	-6.73	0.03	-42.7	0.4	11.1
30	14841	18.03.11	HG drips	-5.96	0.04	-35.8	0.4	11.9
31	14843	18.03.11	HG drips	-5.90	0.06	-35.1	0.4	12.1
32	14847	09.04.11	HG drips	-6.49	0.06	-39.9	0.4	12.1
33	14851	07.05.11	HG drips	-6.67	0.03	-41.3	0.4	12.1
34	14907	18.06.11	HG drips	-6.83	0.05	-42.5	0.4	12.2
35	14912	10.09.11	HG drips	-7.07	0.04	-43.0	0.5	13.5
36	14919	15.10.11	HG drips	-7.26	0.05	-44.7	0.3	13.4

37	14940	23.11.11	HG drips	-6.68	0.03	-41.0	0.2	12.4
38	14930	20.12.11	HG drips	-6.31	0.04	-39.1	0.4	11.4
39	14936	25.01.12	HG drips	-5.91	0.07	-33.5	0.4	13.8
40	14760	15.05.12	HG drips	-6.33	0.07	-34.9	0.2	15.8
41	22566	11.08.12	HG drips	-6.90	0.02	-41.6	0.8	13.7
42	22575	08.09.12	HG drips	-6.72	0.03	-42.4	0.6	11.3
43	19777	08.09.12	HG drips	-6.77	0.04	-41.5	0.3	12.6
44	19778	08.09.12	HG drips	-7.02	0.03	-45.3	0.2	10.9
45	19781	21.01.13	HG drips	-5.71	0.05	-32.6	0.3	13.0
46	19782	21.01.13	HG drips	-5.00	0.03	-29.5	0.2	10.5
47	22561	21.01.13	HG drips	-5.80	0.03	-32.7	0.3	13.7
48	Breit-10	01.03.13	HG drips	-5.97	0.01	-33.8	0.0	13.9
49	24653	23.05.13	HG drips	-6.26	0.03	-38.7	0.3	11.4
50	24674	23.05.13	HG drips	-6.31	0.03	-38.8	0.3	11.7
51	24676	23.05.13	HG drips	-6.54	0.07	-41.2	0.4	11.1
52	28159	24.08.13	HG drips	-6.89	0.03	-43.0	0.2	12.2
53	24743	24.08.13	HG drips	-6.92	0.04	-42.5	0.2	12.9
54	24744	24.08.13	HG drips	-7.07	0.02	-43.4	0.2	13.1
55	24659	26.09.13	HG drips	-7.02	0.02	-43.9	0.5	12.3
56	24686	02.11.13	HG drips	-7.09	0.01	-44.5	0.3	12.3
57	24689	02.11.13	HG drips	-6.52	0.06	-40.1	0.4	12.1
58	24666	27.12.13	HG drips	-6.30	0.03	-36.6	0.3	13.8
59	28146	03.03.14	HG drips	-6.75	0.05	-42.4	0.3	11.5
60	28173	03.03.14	HG drips	-6.87	0.04	-43.2	0.3	11.8
61	28176	03.03.14	HG drips	-5.54	0.03	-32.4	0.4	12.0
62	28154	10.03.14	HG drips	-5.89	0.02	-34.6	0.5	12.6
63	14842	18.03.11	CH drips	-6.24	0.05	-38.2	0.6	11.7
64	14845	18.03.11	CH drips	-5.37	0.06	-30.3	0.4	12.6
65	14849	09.04.11	CH drips	-6.25	0.04	-37.7	0.2	12.2
66	14903	07.05.11	CH drips	-6.58	0.06	-39.8	0.5	12.8
67	14908	18.06.11	CH drips	-6.63	0.06	-40.5	0.4	12.5
68	14913	10.09.11	CH drips	-7.00	0.04	-42.9	0.3	13.1
69	14920	15.10.11	CH drips	-6.96	0.05	-41.9	0.3	13.7
70	14926	23.11.11	CH drips	-6.66	0.05	-41.1	0.6	12.1
71	14931	20.12.11	CH drips	-6.21	0.06	-37.5	0.2	12.2
72	14935	25.01.12	CH drips	-5.69	0.05	-32.3	0.4	13.2
73	16632	15.05.12	CH drips	-6.52	0.04	-37.8	0.3	14.4
74	22578	08.09.12	CH drips	-6.43	0.04	-38.7	0.5	12.8
75	22571	08.09.12	CH drips	-6.34	0.01	-38.4	0.6	12.3
76	22573	15.09.12	CH drips	-6.65	0.04	-40.8	0.4	12.3
77	19783	21.01.13	CH drips	-5.53	0.04	-30.3	0.3	13.9
78	Breit-6	01.03.13	CH drips	-5.75	0.03	-32.2	0.1	13.8
79	Breit-7	01.03.13	CH drips	-5.23	0.03	-26.5	0.0	15.3

80	24898	23.05.13	CH drips	-5.73	0.03	-33.6	0.3	12.2
81	24677	23.05.13	CH drips	-5.72	0.01	-34.1	0.2	11.6
82	24678	23.05.13	CH drips	-5.69	0.04	-34.0	0.2	11.5
83	24650	24.08.13	CH drips	-6.82	0.03	-42.4	0.3	12.2
84	24690	24.08.13	CH drips	-6.92	0.05	-40.5	0.5	14.8
85	24742	24.08.13	CH drips	-6.92	0.03	-42.9	0.3	12.4
86	24658	26.09.13	CH drips	-7.00	0.04	-44.3	0.2	11.7
87	24685	02.11.13	CH drips	-7.27	0.01	-46.0	0.4	12.1
88	24688	02.11.13	CH drips	-6.78	0.01	-41.5	0.3	12.7
89	24663	27.12.13	CH drips	-6.46	0.03	-39.5	0.2	12.1
90	28149	03.03.14	CH drips	-4.59	0.03	-23.4	0.2	13.3
91	28145	03.03.14	CH drips	-6.79	0.04	-40.8	0.2	13.4
92	28147	03.03.14	CH drips	-6.74	0.05	-42.1	0.3	11.9

**Table 2 Concentrations of CO<sub>2</sub> in surface, soil and cave air.** The table is sorted by sampling location. Note that automatic CO<sub>2</sub> logger data is available in supplemental table 1.

Date	Location	Sample type	Sampling method	CO <sub>2</sub> [ppm]
09.01.10	Cherra Resort	Surface air	Air bag	503
12.01.10	Cherra Resort	Surface air	Air bag	481
09.01.10	Entrance	Surface air	Spot analysis	390
13.02.10	Entrance	Surface air	Air bag	527
18.04.10	Entrance	Surface air	Air bag	442
10.01.10	GPD	Surface air	Spot analysis	370
09.04.09	Cave	HG	Spot analysis	490
09.01.10	Cave	Streamway	Spot analysis	400
09.01.10	Cave	Streamway	Spot analysis	400
09.01.10	Cave	CH	Air bag	515
09.01.10	Cave	CH	Spot analysis	560
09.01.10	Cave	CH	Spot analysis	500
09.01.10	Cave	HG	Spot analysis	370
09.01.10	Cave	HG	Air bag	500
10.01.10	Cave	Streamway,	Spot analysis	370
13.02.10	Cave	HG	Air bag	534
18.04.10	Cave	HG	Air bag	443
18.04.10	Cave	CH	Air bag	876
23.05.10	Cave	CH	Air bag	524
07.02.11	Cave	CH	Air bag	485
07.02.11	Cave	HG	Air bag	505
15.05.12	Cave	HG	Spot analysis	1049
13.02.10	Soil	25 cm	Air bag	446
18.04.10	Soil	25 cm	Air bag	441
13.02.10	Soil	75 cm	Air bag	468
18.04.10	Soil	75 cm	Air bag	442
23.05.10	Soil	75 cm	Air bag	481
09.02.11	Soil	75 cm	Air bag	5936

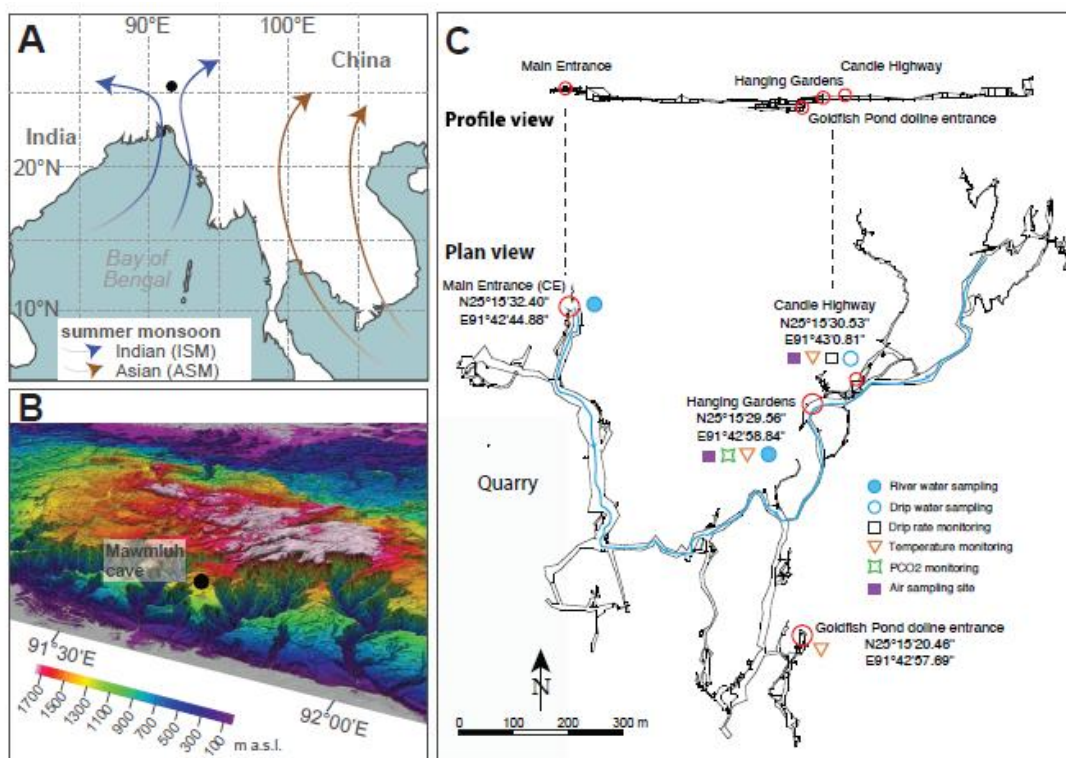


Figure 1

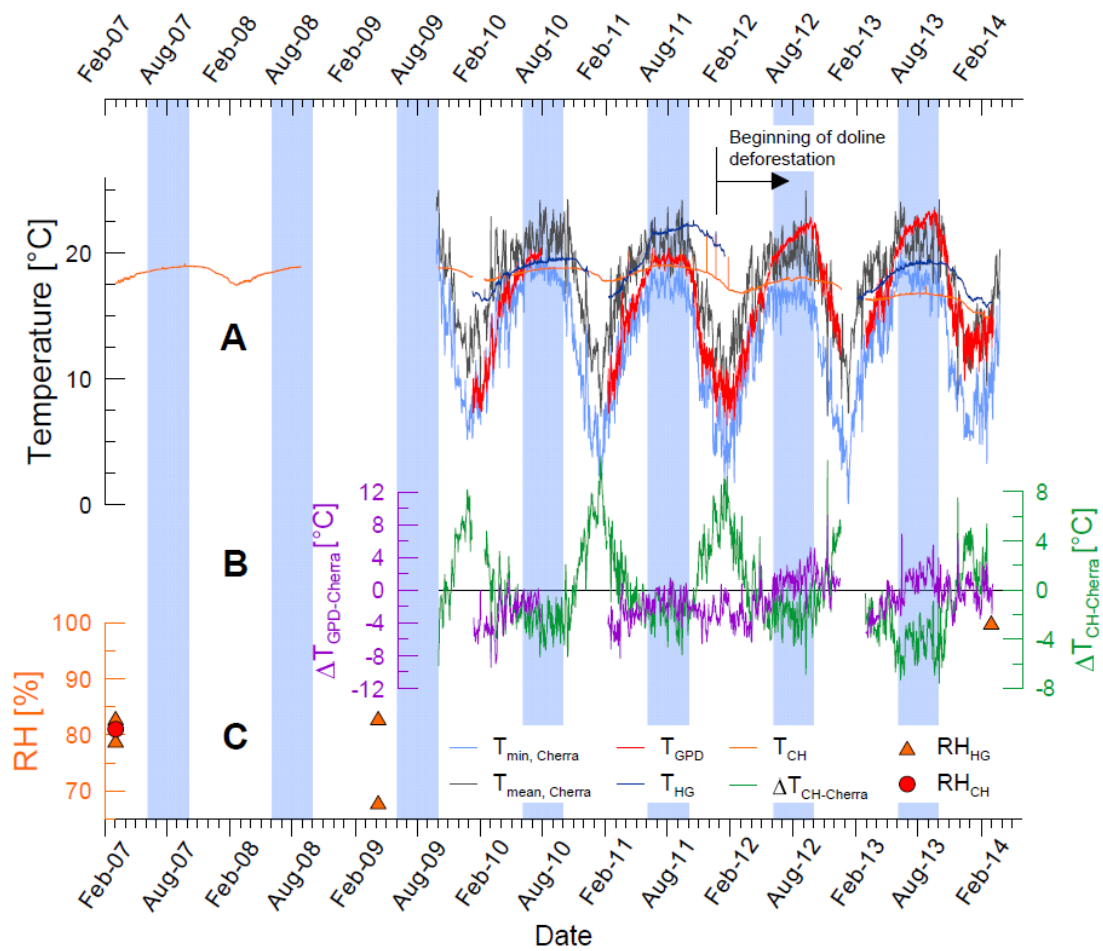


Figure 2

ACCEPTED

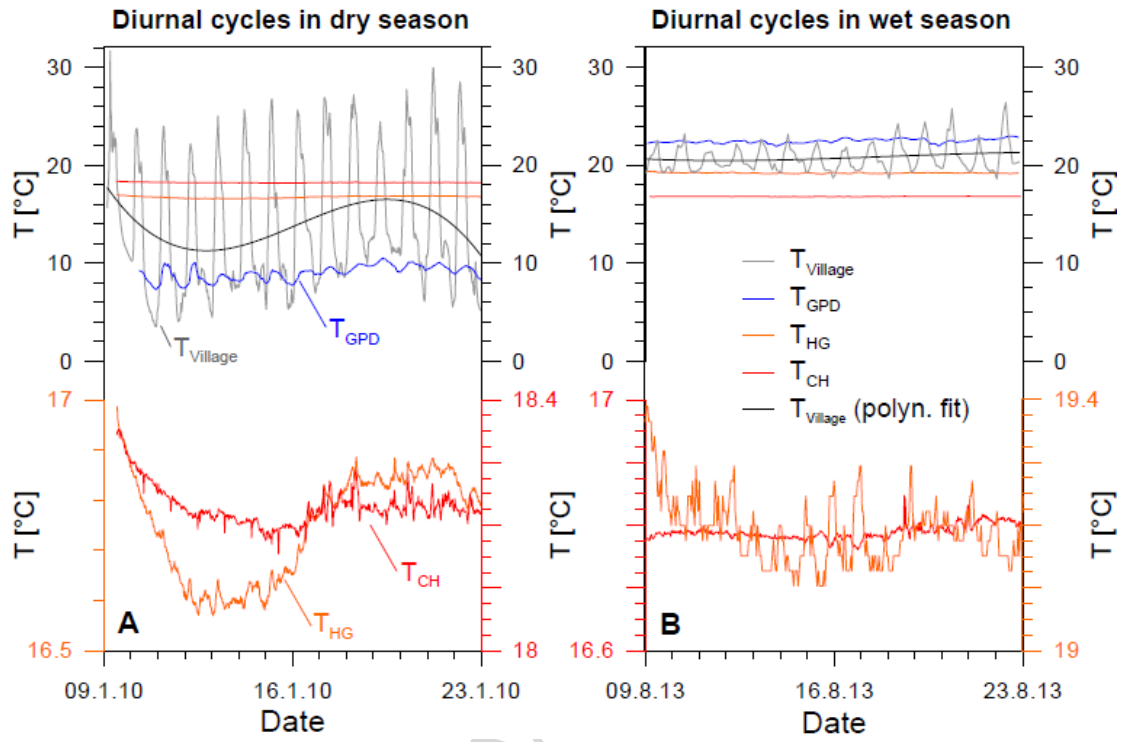


Figure 3

ACCEPTED MANUSCRIPT

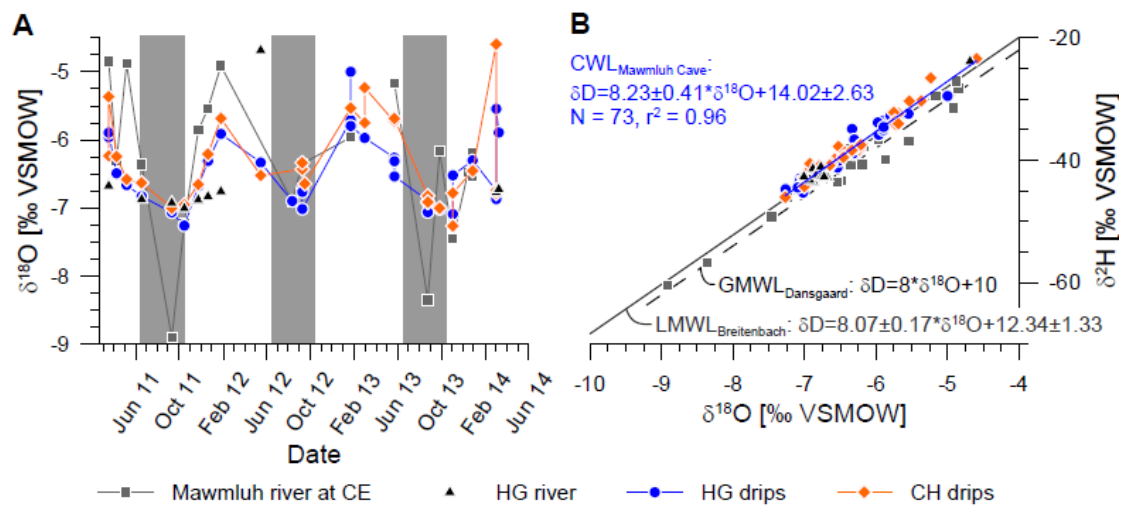


Figure 4

ACCEPTED MANUSCRIPT

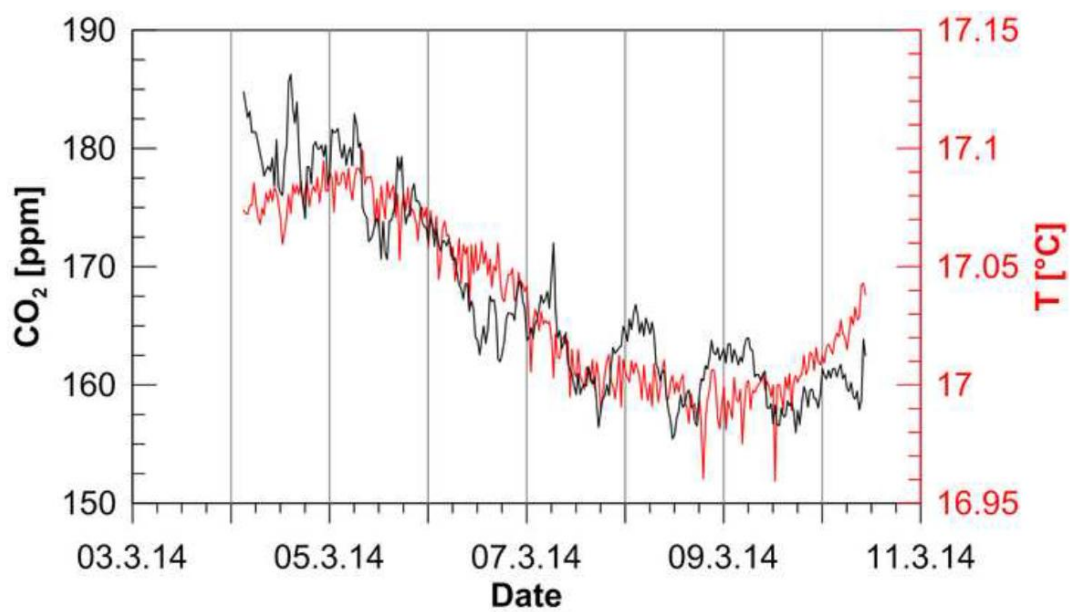


Figure 5

ACCEPTED MANUSCRIPT

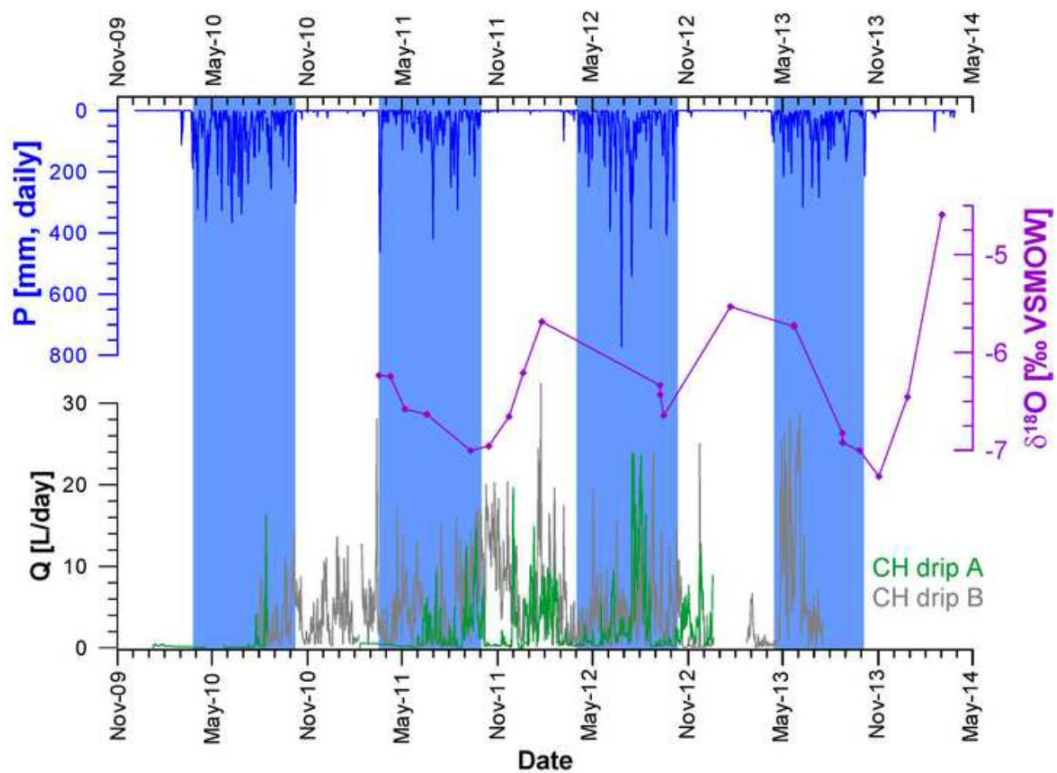


Figure 6

ACCEPTED

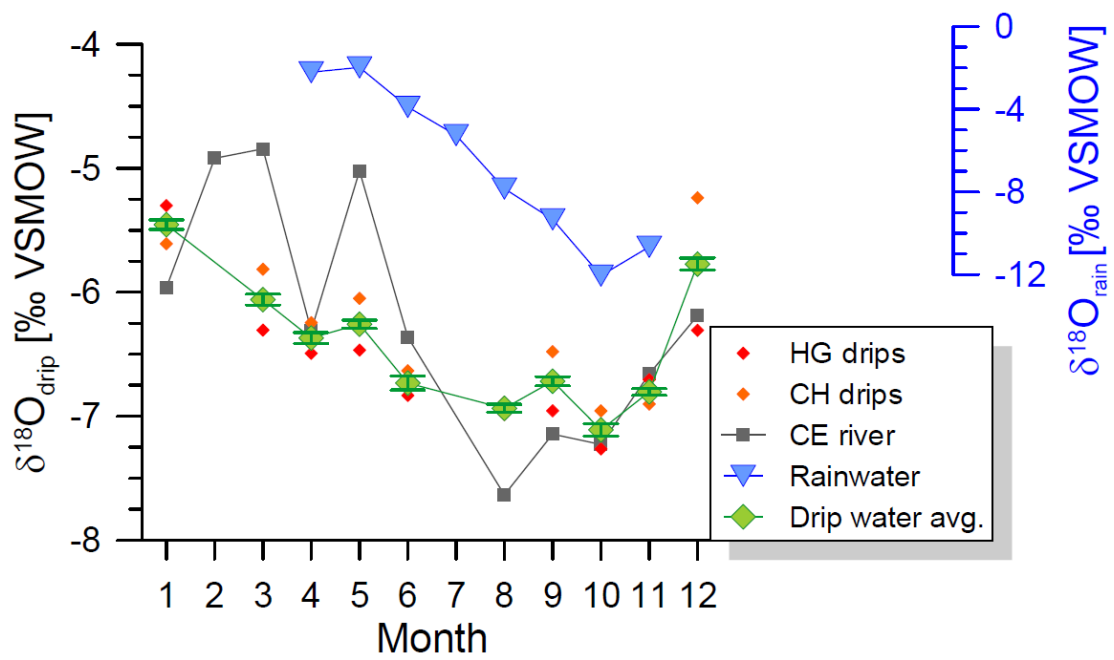


Figure 7

ACCEPTED MANUSCRIPT

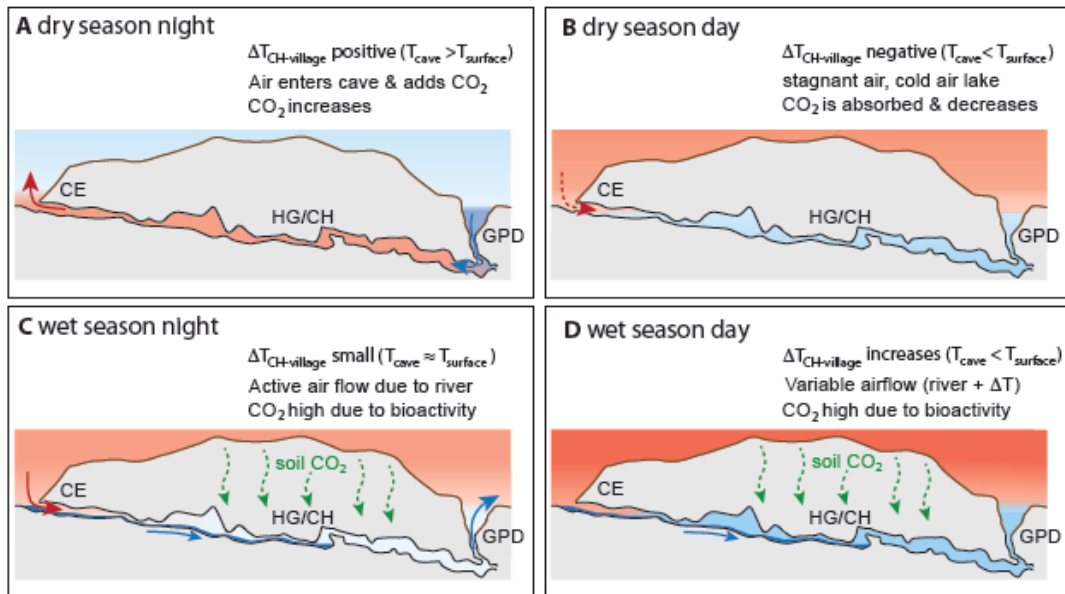


Figure 8

ACCEPTED MA

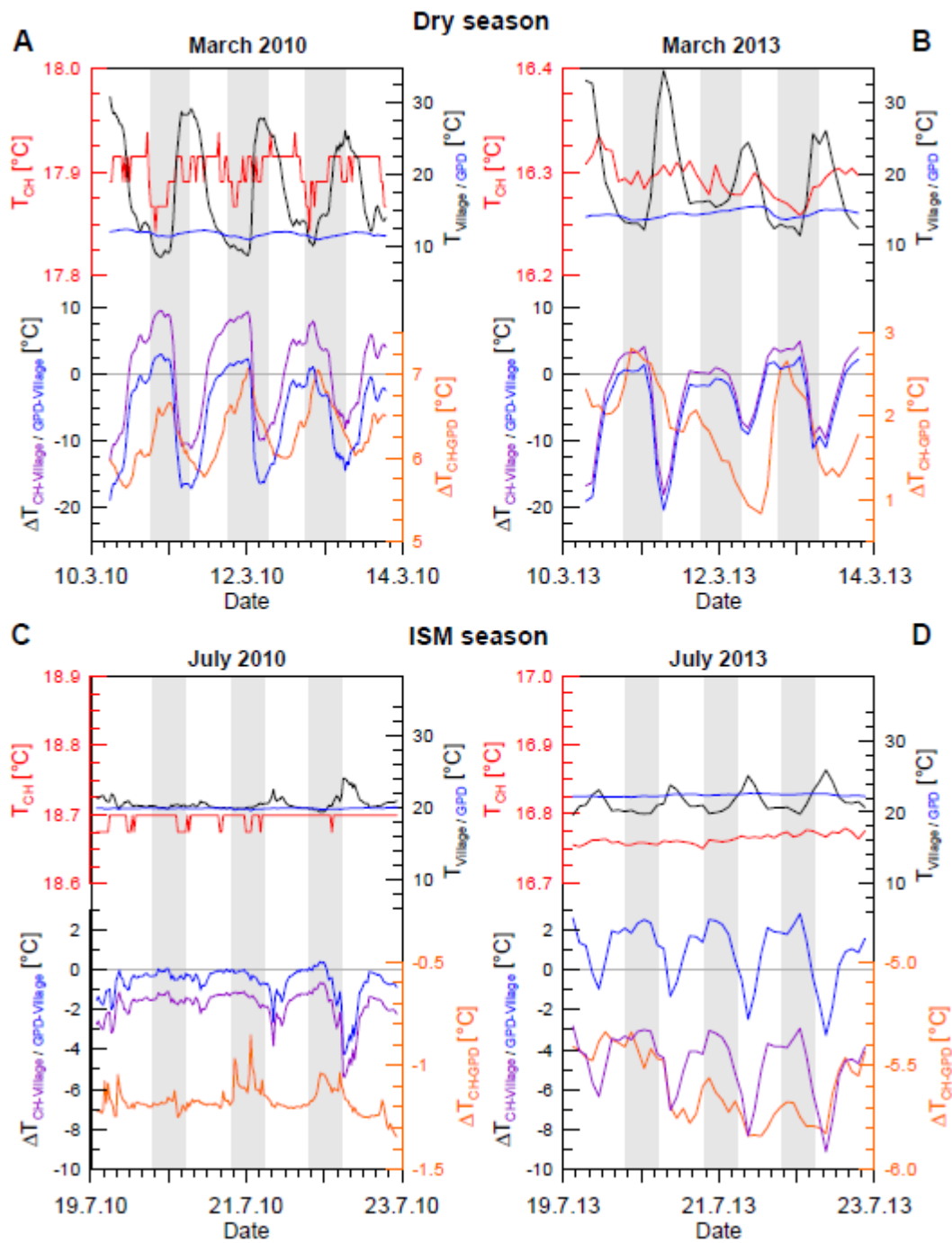


Figure 9

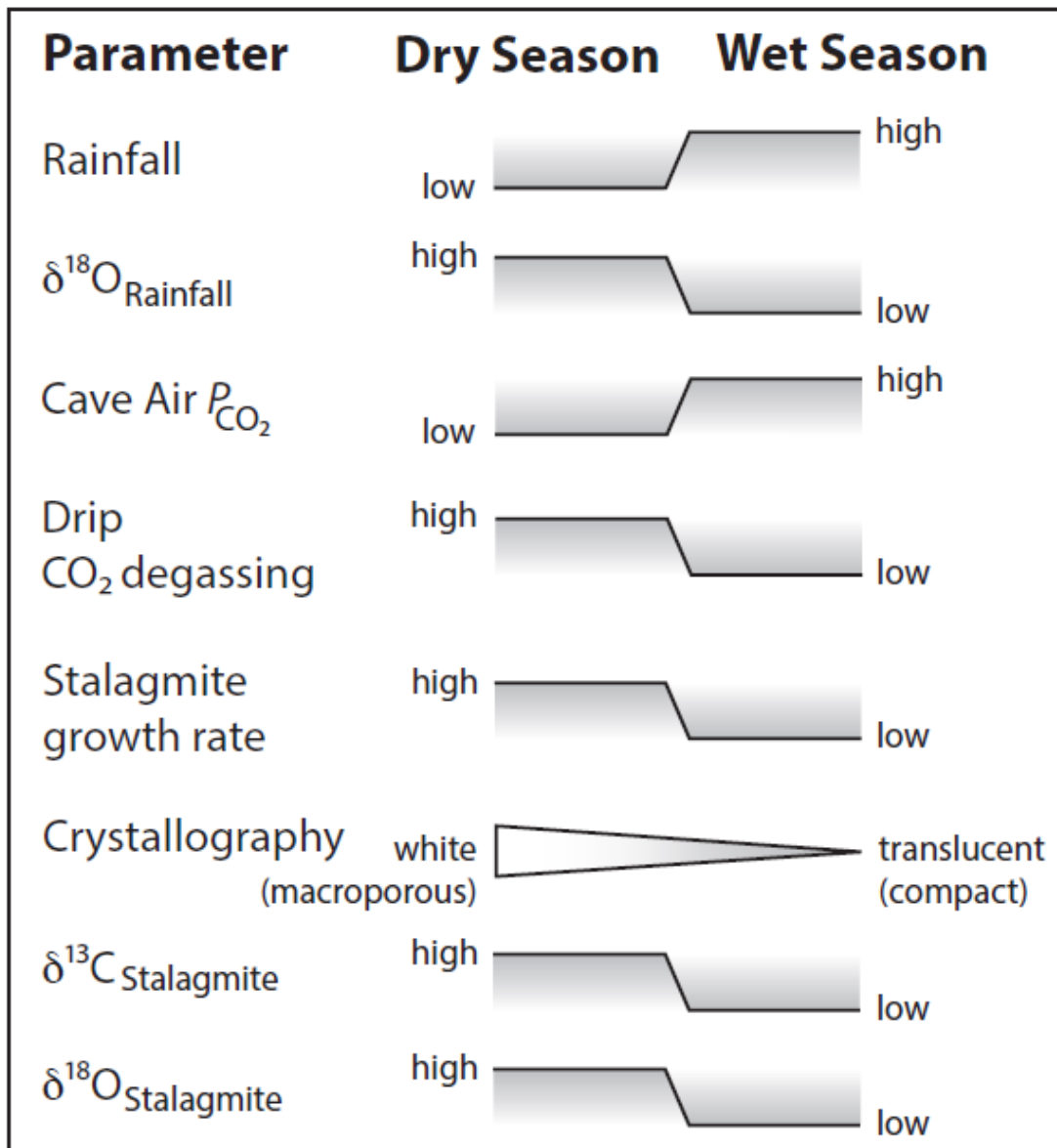


Figure 10